PERFORMANCE AND EVALUATION OF TITANIUM NITRIDE COATINGS

A THESIS

Presented to

The Faculty of the Division

of Graduate Studies

By

Neil W. Sollenberger

In Partial Fulfillment

of the Requirements for the Degree

Master of Science in

Mechanical Engineering

Georgia Institute of Technology

September, 1978

PERFORMANCE AND EVALUATION OF TITANIUM NITRIDE COATINGS

Approved:

Carl H. Jacobs, Chairman

John T. Berry

S. Ramalingam

Date approved by Chairman: 12/4/78

ACKNOWLEDGMENTS

I would like to express my sincere gratitude to Dr. S. Ramalingam for his continuous guidance and patience. The state of development achieved in this study was influenced by his insight and experience. A special thanks is expressed to Dr. Ramalingam for his personal interest which has contributed significantly in my professional development.

To Vermont American Corp., Louisville, Kentucky, I would like to extend my sincere thanks for the financial support of this project.

My special thanks are extended to Dr. Carl Jacobs, faculty advisor, for his friendship and encouragement. His guidance and personal understanding was greatly appreciated. I would like to express my gratitude to Dr. John Berry for general assistance and to Dr. Stephen Spooner for help in obtaining the x-ray diffraction data. I am thankful for their friendship, interest and enthusiasm.

My thanks are extended to Dale Liao, my fellow graduate student, whose curiosity and persistance was very much appreciated.

I am very grateful to my parents and parents-in-law for their interest, love, and encouragement during the course of this work. Special thanks are given to my brother, Craig, for his assistance in drafting many of the figures in this thesis.

I would like to express deep and enduring gratitude to my wife, Gail, for the love and unfailing encouragement given to me during the course of this study.

TABLE OF CONTENTS

LIST OF TABLES

LIST OF ILLUSTRATIONS

Figure Page

SUMMARY

Coatings of Titanium Nitride (TiN) on tungsten carbide inserts can enhance the life of cutting tools in metal machining due to the higher crater wear resistance of TiN when machining ferrous alloys. A satisfactory method for the deposition of thin films of TiN on carbide substrates is however necessary to produce commercially acceptable coated tools.

Sputter coating in the presence of a transverse magnetic field offers an attractive means of attaining this goal. This technique permits coatings to be produced at higher rates. It also permits sputter cleaning of the substrate prior to film deposition to assure the production of adherent coatings.

A magnetron sputter coating system was therefore constructed and an attempt was made to produce TiN coatings on carbide substrates by reactive sputtering. The coated tools produced were used to machine hot rolled AISI 1045 steels in a 10 hp lathe at cutting conditions comparable to those in industrial machining practice to evaluate the performance characteristics of the coated tools. To unambiguously document the enhanced crater wear resistance of the coated tools, a carbide substrate (94WC-6Co) prone to severe cratering when steels are machined, was used.

Machining tests carried out show that TiN coated tools

are superior to uncoated tools and that it is feasible to use sputtering processes to produce reliable and adherent coatings of TiN on carbide substrates which are suitable for metal machining.

In this work the coating characteristics of the sputtering system constructed, in the conventional sputtering mode and in the reactive sputtering mode, are examined. Coating rates and uniformity are evaluated. Possible reactive sputtering modes are discussed and coating conditions under which TiN layers may be produced are identified. Formation of TiN coatings on carbide substrates is verified by x-ray diffraction analysis and documentation in support of this is presented. Details of the performance tests carried out to establish the superiority of the coated tools and the test results obtained are also presented.

CHAPTER I

INTRODUCTION

Background

The sputtering process has been studied for a variety of reasons. It is involved in thermo-nuclear fusion plasmas, erosion of satellite surfaces and ion-propulsion electronics, ion getter pumps, preparation of atomically clean surfaces, etching, and most widely in the deposition of films and coatings. As early as 1877 sputtering was used for coating mirrors. With the development of vacuum technology, sputtering was replaced by faster vacuum evaporation processes. Through the better understanding of sputtering and because of inventions such as radio frequency (RF) sputtering of insulators the advantage of sputtering becomes more apparent.

Sputtering is very compatible and applicable to various materials and is especially well suited for depositions of multilayer devices, e.g. integrated circuits. There has been success in sputter depositing films of complex materials such as stainless steel and pyrex glass, without compositional changes. Film thickness is easily controlled because the deposition rate is constant for conditions of constant voltage, current, pressure, and target material. The uniformity of the deposited film can be improved by increasing the size of the target and substrate rotation. The target,

substrate arrangement is not restricted with respect to gravitational forces, downward sputtering simplifies substrate mounting. One target is sufficient for many depositions. Substrates can be cleaned by back sputtering before coating, and while coating a negative bias can be applied to the substrate for the removal of oxide films. These are some of the advantages of the sputtering technique. Some of the more recent advances will be discussed later (see Chapter II).

The largest demand for sputtered films came from the electronics industry which needed high quality, chemically pure, thin films. The increased demands of micro-circuitry caused sputtering techniques to mature rapidly. Now that sputtering is fairly well understood and has been proved capable of mass-producing repeatable high quality films, other industries have developed an interest in using it for the deposition of high quality films. The cutting tool industry has just recently begun extensive studies on the sputtering process as a technique for depositing TiC and TiN on metal cutting tools.

Much of the increased interest in sputtering has come from the improved quality of the films and the demonstrated feasibility of composite structures (films on substrate). Thin films can be used for many purposes: to provide resistance to abrasive wear, corrosive wear, diffusive wear, radiation damage, and high temperature oxidation; to reduce friction or electrical resistance; to provide lubrication and

prevent sticking, to provide magnetic or dielectric properties, and also for decorative purposes. Because of these desirable properties thin films have been used in electronic, engineering, optical, biomedical, nuclear, space, and other applications. The characteristics and performance of thin films depend on the adhesion between the coating and the substrate. In machining applications the importance of adhesion is greater because when large particles or flakes of the coating are formed due to poor adhesion they could act in an abrasive manner and accelerate the wear of the surface it was intended to protect [1].

Adhesion is very dependent on the coating-substrate system. The transition between the substrate material to the coating usually involves an abrupt change in properties such as hardness, coefficient of thermal expansion, thermal conductivity, etc. These differences in properties cause internal stresses which can cause coating failure, especially when the temperature changes from that of deposition temperature.

There are other factors which affect the adhesion of coating which are not dependent on the coating-substrate system. Poor adhesion can be caused by chemical attack of the substrate surface during the deposition process. Oxide films or other contaminants are usually present on the surface of many metal substrates during deposition, which causes adhesion problems. Many coatings are produced

at elevated temperatures which activate carbon diffusion in carbon-containing substrate materials. This produces a brittle and porous zone between the substrate and coating that results in reduced bonding strength [2]. Taking the above factors in consideration along with cost and reliability of the system, the most advantageous deposition technique can be selected.

By using a substrate-coating combination the properties of the composite product can be greatly enhanced. In the case of cutting tools the substrate can have the strength and fracture toughness required in the cutting process while the coating can be of hard, high temperature wear resistant material. This idea was introduced almost ten years ago with the TiC and TiN coated tungsten carbide inserts. The coating process utilized is the conventional chemical vapor deposition, CCVD. This process, however, is not practical for coating high speed steel tools and has had adhesive problems due to the elevated temperature at which the coating process is carried out.

There are many techniques which are being developed for depositing TiC and TiN on different types of substrates. Most of the techniques are of a chemical vapor deposition type, while at least one technique is a physical vapor deposition. The chemical vapor deposition technique is defined as the deposition of a solid material onto a substrate surface, which is usually heated. The chemical

reactions occur primarily in the gas phase [3]. The processes are generally differentiated by three parameters: principal mode of activation of the chemical reactants; mode of transport of the chemicals; and initial state of the gaseous chemical reactants. Physical vapor deposition is a sputtering process where atomic deposition of the target material occurs due to ionic bombardment.

The chemical vapor deposition (CVD) techniques include: conventional CVD, reactive evaporation (RE), activated reactive evaporation (ARE), reactive sputtering, magnetron reactive sputtering (MRS), and reactive ion plating (RIP). A brief description, advantages and disadvantages and results of previous experiments using CVD techniques is presented below.

The process which has been used commercially for coating tungsten carbide tools with titanium carbide and nitride is convention chemical vapor deposition (CCVD). The advantages obtained from the coated carbides is not only increased tool life, but also increased machining speed for the same tool life as that of uncoated tools, and reduced cutting forces due to lower friction.

CCVD are a process in which gaseous chemical reactants are activated thermally by the heated substrate and made to react to form a solid deposit on the substrate surface. The reaction equation for TiC and TiN are

$$TiCl_4 + CH_4 \rightarrow TiC + 4HCL$$

$$TiCl_4 + 2H_2 + 1/2\ N_2 \rightarrow TiN + 4HCL$$

respectively. The deposition rate is affected by temperature, pressure, composition of the gas, etc., where temperature has the greatest influence. At temperatures of about 1000°C the coating rates for TiC is about 1.5 microns per hour [4], and 8 microns per hour for TiN [5]. Kieffer, et al. observed that the TiN coated carbide had a 3-5 times better cratering resistance than TiC coated carbides [5]. They also found that wear resistance falls drastically for TiN coatings coated at temperatures under 1000°C. Therefore, CCVD is limited to coating carbide tools and is not practical for coating HSS tools because of the high temperature and because of chemical reaction between HCl and steel.

Reactive evaporation is simply the evaporation of a metal in a reactive environment at low pressures. The typical operating pressure is in the range 1.33×10^{-2} - 1.33×10^{-1} Pa. Itoh [6] used this process in the formation of TiN and ZrN. It was found that the optimum substrate temperature for the formation of TiN and TiC was 320°C to 330°C. The deposition rate was approximately 60 Å per minute and the films were studied for use as electrical resistors.

Activated reactive evaporation (ARE) is essentially a reactive evaporation process with plasma activation [7]. The working pressure is determined by the method of plasma generation; the range of pressure for these methods is usually 1.33×10^{-2} to 1.33×10^{2} Pa. Coating rates for TiC have been as high as 1 to 2 microns per minute when electron beam melting is used with a beam power of 10 KV and 200 MA. The substrate temperature was 700°C to 1000°C. Tungsten carbide tools coated with TiC by the ARE process showed comparable, if not better, wear resistance than commercially available CCVD-processed TiN-TiC composite coating tip in 15 minute machining tests [8]. TiN was deposited on mild steel at substrate temperatures of 150°C to 500°C by the ARE process, but was not tested for wear resistance. Bunshah, et al. [9] coated high speed steel tools (type M42) with TiC using ARE process with substrate temperature of 550°C. The coated tools exhibited a tool life 300-800% higher than the uncoated tools under continuous cutting conditions. The cutting forces were measured and found to be 50% lower for coated tools than for uncoated tools.

Reactive sputtering is the sputtering of a material in a reactive environment. The negatively biased coating material or target is bombarded by positively charged gas ions, inert and reactive. The target material is ejected from the target surface to react with the reactive gas to

form a coating on the substrate. Straight d.c. reactive sputtering process operates typically at several kilovolts, with a gas pressure from 1 to 7 Pa. In the past the coating rates were low (~1 micron per hour) at relatively high pressures, but with the development of the magnetron sputtering system the coating rates at pressures of 0.4 Pa are comparable to that of ARE process. Clarke has obtained TiN coating by using the magnetron d.c. reactive sputtering [10], but no cutting tools have been coated by this method at the present time (1978).

Reactive ion plating is a combination of ion plating and ARE. TiN films have been produced by RF reactive ion plating, but at coating rates of 300 Å per minute [11], which is very slow compared to other techniques, so will not be discussed any further.

Within the last six years there has been an increased interest in the development of the sputtering process for coating tungsten carbide (WC) and HSS tools with TiC and TiN. In 1973 Mah, et al. [12] used a triode sputtering process for coating TiC and TiN on tungsten carbide tools. The deposition rate was 3 microns/hour at target voltage of 1 KV and 100 MA, filament voltage of 15 V and 90 A and pressure of 0.267 Pa. The sputtered TiC coatings were found to provide the same improvements to the WC tools as in the case of CCVD coatings. Cook and Su [13] coated HSS cutting tools with TiN by using the RF sputtering technique.

The deposition rate was 1 micron per hour with the substrate at ground potential, argon pressure of 0.533-1.333 Pa, and at 750 RF watts with corresponding target potential of 3150 volts. The tool life was increased 2-4 times and the cutting forces and friction coefficients were significantly lower for the TiN coated tools when compared to the uncoated tools. Additional studies have been carried out which indicate that adhesion of TiC RF sputtered coating on steel substrates have been excellent and can be increased by biased sputtering which causes a chemically mixed film-substrate interfacial region [14,15]. Also it has been found that the adhesion is dependent on the sputter gas pressure [1,16].

A comparison of the deposition techniques given in Table 1 shows that all but CCVD can be readily used for various substrates. The ARE and MRS techniques are definitely ahead in the deposition rate and are comparable in all categories except substrate preparation. The MRS process has the ability to sputter clean the substrate to remove the oxide and other contaminant films before the deposition which would improve adhesion between the film and substrate.

Objectives of this Research

Recently, there has been a rapid improvement in the technology and understanding of the magnetron sputtering

Table 1. Summary of Deposition Techniques

Deposition Technique	Deposition Rate	Substrate Temp.	Reactive By-Prod.	Deposition Pressure	Substrate Prep. or Cleaning	Ref.
CCVD	1-8 microns/hr	1000 C	HCl	13-133 Pa	Heat	4,5
Reactive Evap.	.1 microns/hr	100-1000 C	None	.013-133 Pa	Heat and Low Pressure	6
Activated Reactive Evap.	60 microns/hr	100-1000 C	None	.013-133 Pa	Heat, Low Pressure, & Pre-coating	7,8, 9
Reactive Sputtering	.1-5 microns/hr	100-500 C	None	1.3-13.3 Pa	Sputter Cleaning	38, 40
Magnetron Reactive Sputtering	30-60* microns/hr	100 C	None	.07-2 Pa	Sputter Cleaning	10, 50
Reactive Ion Plating	.03-1 microns/hr	100 C	None	1-7 Pa	Sputter Cleaning	11
RF or Triode Sputtering	1-5 microns/hr	100-500 C	None	1-7 Pa	Sputter Cleaning	12, 13

*Deposition rates based on dc magnetron sputtering.

system [17,18]. This development has revolutionized the sputtering technique because it has increased the deposition rate by over a magnitude along with lower deposition pressures at voltages of only 500 V to 800 V. Benefits of the magnetron sputtering system include reductions in substrate heating, radiation damage and film contamination. It is suited for operation in modes that result in lower coating costs. By using in-line production magnetron sputtering the deposition of multilayer films onto moving substrate simplifies the problem of attaining uniformity and, at the same time, provides high production rates [19].

Very few reports have been published on the use of magnetron sputtering system for the reactive sputtering process. The objectives of this research is to develop a high rate planar magnetron sputtering system to be used in the reactive sputtering of TiN on tungsten carbide insert tools. The coated insert tools are then to be compared to uncoated tools in machining tests for wear resistance.

The first step of this study is to develop a planar magnetron system such that the sputtering of titanium can be done with an applied target power density of 70 to 100 W/cm^2 at argon pressures of 0.13 to 0.4 Pa. Once that is accomplished the sputtering of titanium in an argon and nitrogen environment will be studied by varying the partial pressure of nitrogen, current, total pressure of the sputtering environment, substrate heating, and biased sputtering.

After looking at these variables, the coating conditions will be selected for coating the tungsten carbide tools.

CHAPTER II

LITERATURE REVIEW

History of d.c. Sputtering

Sputtering is the occurrence of atomic ejection from the surface of a solid due to the collision of single atoms, ions, or molecules. The processes that occur when a particle bombards the surface of a metal or other material is *dependent upon the kinetic energy of the bombarding particle.* If the collision occurs with a particle of low kinetic energy, the interaction is at the outer most surface and collisions can cause the emission of secondary electrons. As the kinetic energy is increased, the bombarding atoms actually knock atoms into new positions and cause surface damage due to surface migration. As bombardment continues, some atomic ejection can occur due to the surface damage. Increasing the kinetic energy even further, the target atoms become dislodged into the gas phase much more readily. It is the atomic ejection of the second and final stages which is considered sputtering.

The first report of the observation of sputtering of a cathode in a glow discharge was by W. R. Grove in 1852 [20]. It was his objective to show that gases do not conduct electricity in any manner similar to metals or electrolytes.

He discovered that plates which were separated from a wire in an air vacuum, with an applied voltage potential between them, would form spots of oxidation which were apparently eroded into the plate. In a hydrogen environment vacuum, the plate did not oxidize, but a surface change was perceptible, producing a "frosted appearance." When previously oxidized plates were placed in the hydrogen environment vacuum and the experiment repeated, the oxidation was rapidly removed. In other experiments a glow discharge which he called "a cone of a blue flame" was observed. He also observed a dark space in the glow discharge. In some experiments which were continued for sometime, dark deposits were observed.

When using sputtering for the purpose of producing thin films, the technique used to obtain the kinetic energy required by the bombarding species is by ionizing gas particles. The cathode or target is maintained at a high negative potential with respect to the anode or substrate, both of which are separated in a vacuum (0.133 to 133 Pa). Electrons tend to flow from the cathode to the anode. When the mean free path of the electrons is small compared to the distance between the anode and cathode, the electrons collide with gas molecules. If the electrons have a sufficient energy, they will cause ionization of the gas molecules. The gaseous ion produced is accelerated towards the cathode due to the electrical potential difference. The ionized gas molecule

therefore picks up kinetic energy from the electric field and bombards the cathode.

When a high enough potential is impressed between the anode and cathode, a stable glow discharge can be established. The glow discharge developed depends on several factors: the pressure of the gas, the applied voltage, and the electrode configuration. These factors control the mean free path of the electrons and gas molecules, the energy of the electrons and therefore the chances of ionization upon collision, the overall length of the electron flow and therefore the number of collisions. R. W. Berry [21] showed the current voltage characteristics of a discharge between two flat parallel plates in a gas with pressure of 1 Pa. Initially there is essentially no current until a minimum breakdown voltage is reached. When this voltage is reached the electrons which do flow have sufficient energy to cause ionization, which in turn generate new electrons. When the ionization current reaches significant proportions, the ions tend to accumulate in front of the cathode which produces a localized space charge. Therefore, the electrons have a very high energy coming off the cathode and ionization occurs on the first collision and a glow discharge is established (see Figure 1). After the electrons pass this glow discharge zone, many ion-electron pairs are formed and the potential falls off. Once the glow discharge occurs, the voltage can be lowered below the breakdown voltage while still maintaining

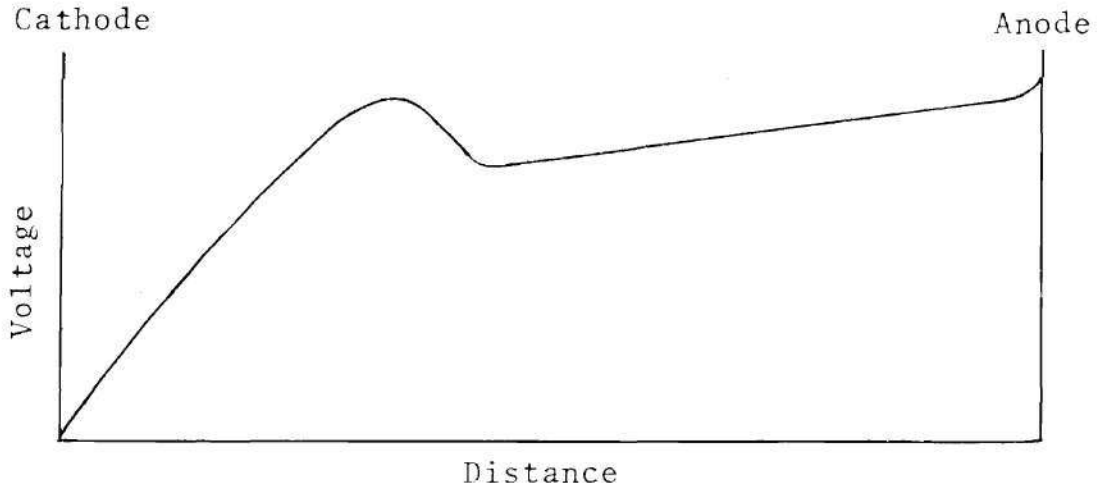

Figure 1. Schematic Illustration of the Voltage-Distance Characteristics of a Glow Discharge Between a Cathode and Anode in Low Pressure [21]

the discharge, because of the immediate high potential between the glow discharge and cathode. When the voltage and the current are further raised, the voltage will drop abruptly and the discharge becomes an arc.

For a more detailed review of the physics of glow discharge see references [21] and [22].

There have been many attempts to develop theories of sputtering. One of the most prominent theories in its time was the "hot spot theory," presented by Von Hippel in 1926. According to Von Hippel the bombarding particle dissipates energy upon collision in the form of heat, the energy being very localized and high enough to cause evaporation of the target atom. Early experiments seemed to confirm this theory

but were misleading. Most of the experiments were done in a glow discharge at pressures of approximately 133 Pa. Under these conditions there was very little control over the mean free path of the electrons or gas particles, ion energy, on angle of incidence of bombarding ion, all of which have an effect on the outcome of the results. An early experiment done by Seeliger and Sommermeyer [23] avoided some of these difficulties by using an ion beam for sputtering. The energies of the ions were very high, 5 to 10 KeV, and the results indicated that the distribution of the sputtered deposits followed a cosine law, irrespective of the angle of incidence. This distribution would be expected in the case of evaporation, and was accepted as a proof of the validity of the evaporation theory of sputtering.

The acceptance of this theory started to change in the 1940's, after Fetz's [24] study on sputtering of wires as a function of wire diameter. He discovered that the sputtering rate[1] or yields[2] were the highest for the wires of smallest diameter and as the wire diameter increased the yield approached the value of a planar target. The explanation of this was the angle of incidence had a major effect on the sputtering process and that sputtering occurred more

---

[1]Amount of material removed per unit time.

[2]Number of sputtered atoms per bombarding ion.

readily when the majority of collisions were oblique from normal. These results could not be explained under the evaporation theory but did support developed theories of momentum transfer. In the 1950's G. K. Wehner noticed this relationship [25] and started experiments along the same lines. He also observed the increasing yield with greater oblique angles of incidence [25,26]. In 1959 Wehner published a paper of greater detail on the angle of incidence effect [27]. Here he showed that the yields of some metals such as gold, silver, and copper were not effected by angle of incidence, but yields of other metals such as iron, tantalum and molybdenum were greatly effected.

R. C. Bradley carried out a study on the sputtering of alkali atoms by inert gas ions of low energy [28]. Some of the conclusions he came to are: at low energy, the sputtering rate can be correlated to the average amount of energy transferred to a single surface atom in a two-body collision, at high ion energy, sputtering rate increases as the mass of the ion increases; no evidence was found to agree with the hot spot theory; and that the rate of sputtering is greatly effected by surface conditions such as oxide layers. Wehner experimented on the same subject as Bradley but in greater detail [26]. He determined the minimum ion energy for sputtering (threshold energies) for twenty-three metals under normal incident Hg ion bombardment. From these experiments he found that the product of the momentum

transferred at threshold from ion to target surface atom and the sound velocity of the target material is proportional to the heat of sublimation of the target material. He also observed that the threshold energies were much lower when the target was under oblique incident ion bombardment. When metal single crystals were sputtered, the ejection pattern was observed to be in the directions of closest packing. These results would agree with the idea that the basic process in sputtering is one of momentum transfer.

For further evidence that sputtering is a momentum transfer process, Thompson [29] bombarded a gold foil which had a strongly preferred grain orientation with high energy protons. He found the gold atoms sputtered from the far side of the foil were ejected in the closest packed directions, which is very similar to the ejection patterns from the front side when bombarded at low energies. Anderson and Wehner [30] studied the atom ejection patterns of single-crystals when sputtered. They found that the patterns supported the concept of focusing collisions in the nearest and next to nearest neighbor directions.

For a better understanding of the sputtering process other areas were studied. In 1961 two papers, one by Laegreid and Wehner [31], the other by Wehner and Rosenberg [32] were published on the sputtering yields as a function of material. It was discovered that the yields increase consistently as the outer d shells are filled, with copper, silver, and gold

having the highest yield. This was found true for both low and high energy ions. These results indicate that as the d-shells filled, the collision between the gas atom and target atom closely resembles that of hard spheres. In the case of materials with less d-shell electrons, the electronic structure is more open, thus the bombarding particles seem to penetrate deeper into the lattice and lose kinetic energy in processes other than sputtering.

In a study to determine the effect of ion element on sputtering, Almen and Bruce [33] measured the sputtering yields for three targets with 45 KeV ions of 70 elements. They found that the maximum sputtering yields occurred for noble gas ions and that for reactive gases such as nitrogen the yields were almost zero. They also noted that the sputtering ratios for related ions increased as the mass number increased.

The conclusion of these experiments is that sputtering is a process of momentum transfer. One belief is that the bombardment is followed by a focusing sequence responsible for ejection of atoms. Others feel the collisions give rise to ejection as a result from glacing "billiard ball" interaction. For more details on the theories which explain the sputtering process the reader should see references [34], [35], and [36].

Reactive Sputtering

There are many advantages to reactive sputtering the process is very versatile. Almost any metal can be

sputtered under appropriate discharge conditions, and almost any gas can be mixed with the inert gas flow. Oxides, nitrides, carbides, sulfides, borides, and silicides are among the compounds which can be deposited by this technique. By utilizing high purity initial materials in the cathode and gases, high purity films can be synthesized. The stoichiometry of the compound can be controlled, which in turn controls the properties of the films.

The mechanism for reactive sputtering is very dependent on partial pressure of reactive gas, proportion of reactive gas, current density, sputtering rate, chamber design, target material, and cathode to anode spacing. The location of the chemical reaction between the reactive gas and sputtered species is very important [37]. When the sputtering rate is low or the reactive gas pressure high, the reaction occurs at the cathode, and sputtering of the compound occurs. The reaction may occur during transport, but the probability is small because of problems of conserving momentum while also dissipating the heat of reaction. The most desirable and most usual process is the reaction occuring at the substrate during deposition.

There have been several studies on the sputtering rate as a function partial pressure of the reactive gas in the plasma [38,39,40]. While sputtering in a reactive environment, an abrupt decrease of the sputtering rate of target materials has been observed at a definite partial

pressure of a reactive gas (see Figure 2). To explain this occurence, three processes may be considered: the change of the average sputtering efficiency of the incident ions with the concentration of the reactive gas, the change in the progress of the surface reaction on the target, the change of the mode of discharge with the concentration of the reactive gas.

During deposition the "gettering" action of the sputtered active atom deposits causes the adsorption of the reactive gas. If the reactive gases cannot be absorbed into sputtered deposits fully, residual reactive gases will impinge on the target and the reaction will proceed on the target surface. Once the reaction starts to occur at the target and the compound layer is formed, the sputtering rate is reduced so as to enhance the target reaction until the compound layer covers the target surfaces completely. This phenomenon is observed as a steplike decrease in the sputtering rate. By using rf reactive sputtering it was observed that the sputtering rate in the reactive environment before the abrupt decrease is approximately the same as the sputtering rate in pure argon environment, while the sputtering rate following the decrease is the same as the sputtering rate of the compound.

Below the critical pressure when a metal film is deposited in a reactive environment, the gas and the film will interact. The three common forms for potential energy

between a gas molecule and solid is shown in Figure 3. Curve I gives the potential energy for physical adsorption, where the interacting forces are Van der Waal forces. Curve II shows the potential energy for chemical adsorption of a diatomic molecule which dissociates upon adsorption (forming two adatoms). Curve III gives the potential energy for a dissociated molecule whose atoms can penetrate the solid by diffusion [41].

The chemisorption is characterized by the fact that the electron shell of the adatom may penetrate that of the metal. Both the metal and the adatom give up an electron with unpaired spin to form a "binding orbital." The metal electron usually comes from the d band* (the 3d, 4d, 5d band, depending on the kind of metal).

In the case of sputtering Ti in an nitrogen and argon environment, as an N_2 molecule experiencing potential I collides with the Ti deposit, it may become trapped or physisorbed in the minimum E_p or it may be reflected back into the gas phase. If the physisorbed molecule receives a certain activation energy required to cross the potential hump between E_p and E_c, it can transfer to the potential II curve on which (after dissociations) its atomic constituents become chemisorbed. Upon receiving more energy the chemisorbed atoms can proceed into the bulk of the film by diffusion.

---

*Titanium--$3s^2$ $3p^6$ $3d^2$ $4s^2$.

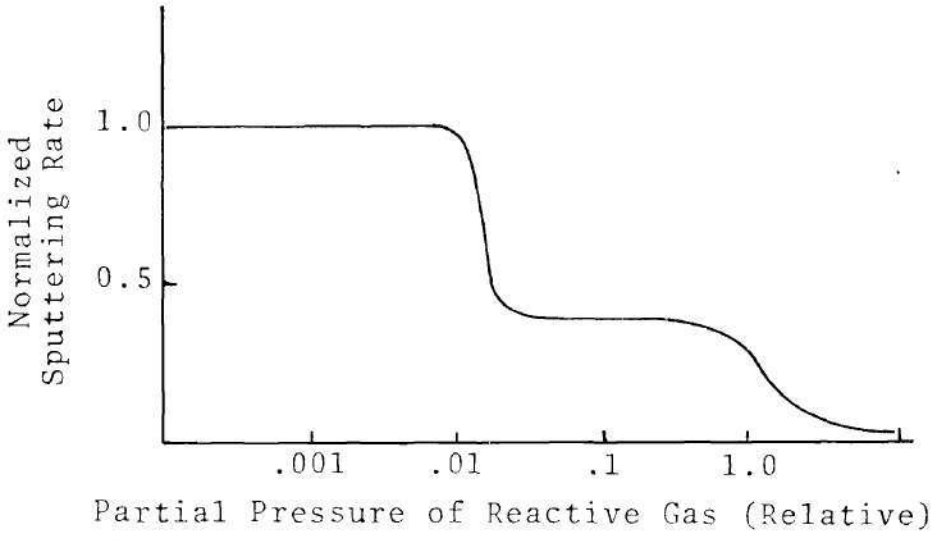

Figure 2. Normalized Sputtering Rate as a Function of the Partial Pressure of Reactive Gas [41]

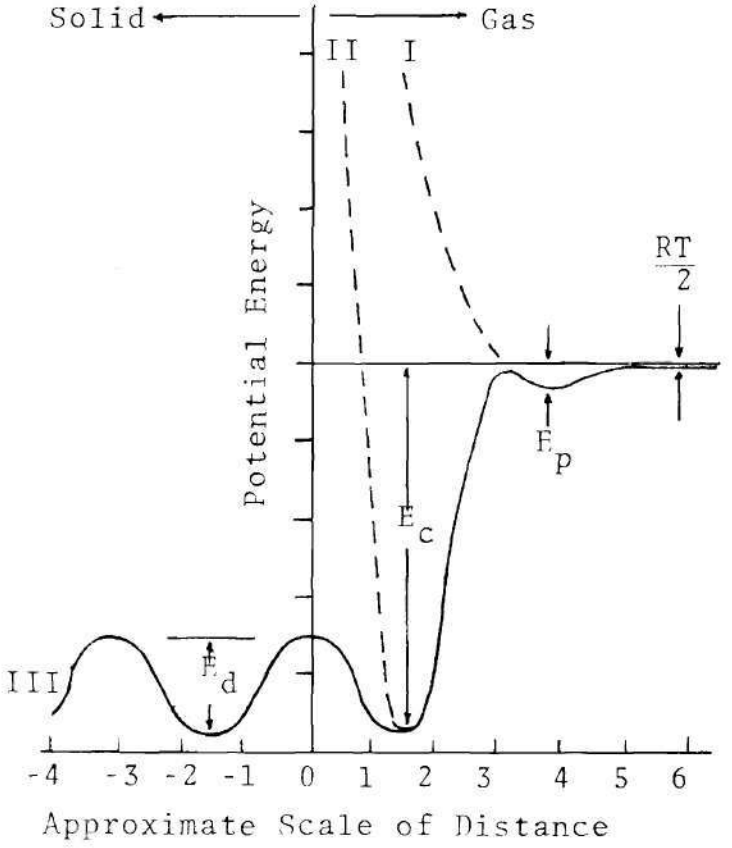

Figure 3. Approximately Representation of Potential Energy Between a Gas Molecule and a Solid Surface. I--Physisorption; II--Chemisorption; III--Diffusion [41].

For a greater, detailed explanation of the reaction between a reactive gas and solid the reader is referred to references [35] and [41].

Hollands and Cambell [40] showed that at any given temperature, and at a constant rate of tantalum deposition, the degree of oxidation of the sputtered films increased with the partial pressure of oxygen. The pressure-dependence suggested that a chemisorption equilibrium precedes the rate-determining step of oxide growth. The adsorption of nitrogen into titanium can be expressed in a similar manner such that

$$\text{site} + \frac{1}{2} N_2 \rightarrow \text{N-chemisorbed} \qquad (1)$$

$$\text{N-chemisorbed} + \text{Ti} \xrightarrow{\text{absorption}} \text{Ti/N} \qquad (2)$$

The concentration of chemisorbed nitrogen atoms can be expressed as

$$[N]_{\text{chemisorbed}} = K\,[N_2]^{1/2}$$

where K is the chemisorption equilibrium constant. Substitution of p/RT for $[N_2]$ ($[N_2]$-concentration) according to the ideal gas laws gives

$$[N]_{\text{chemisorbed}} = \frac{K(P_{N2})^{1/2}}{(RT)^{1/2}}$$

Thus at constant temperature the rate of nitriding formation is approximately proportional to the square root of the nitrogen pressure.

In many cases a series of compounds may be formed, depending on the conditions prevailing during sputtering. Penny and his coworkers [43,44,45] have addressed this problem and correlated the formations of the particular phase with the percentage of reactive gas in the sputtering environment and a quantity E*, called the reduced field, which is given by

$$E^* = \frac{\text{cathode voltage}}{\text{cathode-anode spacing x pressure}} .$$

Clarke [10] used the reduce field and showed that for E* of 8.5 to 9.8 Ti + TiN was formed, for an E* of 7.5 to 8.5 TiN was formed, and for an E* less than 7.5 TiN_x, x>1, was formed. This would indicate that at constant pressure and voltage the rate of adsorption of nitrogen at the substrate surface increases with the increase in the anode-cathode spacing.

Magnetron Sputtering

Many of the earlier experimental results have been obtained while sputtering in a glow discharge of gas pressures where the mean free path of the ions and sputtered atoms is small compared to the chamber dimensions. Under such

conditions it has been found that back-diffusion or ionization of sputtered atoms causes them to return to the target. Difficulties also arise from the formation of impurity surface layers on the target which decrease sputtering yields. The simple solution to these problems is to sputter at lower gas pressures, but by lowering the pressure, the ionization collisions decrease until the glow discharge cannot be sustained. Two techniques have been developed which allow sputtering to occur at low gas pressures. One technique, known as triode sputtering, utilizes an electron emitter to increase the electrons and hence ion populations in the plasma. The second development, known as magnetron sputtering, uses a magnetic field to increase the number of ionizing collisions of the existing electrons by increasing their overall path length.

Penning and Moublis [45] recognized the very important concept of using a magnetic field to help support the glow discharge as early as 1939. Using the magnetic field they were able to maintain a glow discharge at a pressure of 0.133 Pa. The full impact of the use of magnetic fields for increasing sputtering rates at lower pressures was not fully realized until recently.

When an electron moves with a velocity, v, in a vacuum perpendicular to a uniform magnetic field B, there is a force exerted onto the electron,

$$F = e \cdot \vec{v} X \vec{B}$$

where e is the charge of the electron. This force, known as the Hall force, is exerted at right angles to the direction of motion of the electron and acts as a centrifugal force constraining the electron to travel in a circular path. By applying a magnetic field near the cathode surface such that it is perpendicular to the electron flow, the electrons will be forced to flow in spiraling paths. The net effect is an increased path length and therefore the number of ionization collisions is increased. Once the glow discharge is established, the electric field between the cathode and anode (see Figure 1) determines the motion of the electrons. In the magnetron Penning designed, a magnetic field is applied parallel to a cylindrical cathode. In the sputtering mode of this system, the electrons are forced to travel small cycloidal paths in large circles around the cylinder axis. An electron continues along this path until collisions are made with the gas. The electron then drifts closer to the anode [17,18,46]. Because the electrons must undergo ionizing collisions before escaping, the gas discharge can be sustained at very low gas pressures with very high current densities.

Chapin [46] developed a technique for applying a magnetic field to a planar target which obtains the Hall drift in a closed loop. If a magnetic field is applied

parallel to a planar cathode, the Hall drift carries the electrons off to one side. If the magnetic field comes out of the cathode from its outer periphery, becomes nearly parallel to the cathode, and then goes back into the cathodes' center region, a closed loop will be formed so that the Hall drift will carry the electrons round and round. From this design very large discharge currents similar to the Penning device can be obtained.

The magnet arrangements have been varied substantially in the designs of magnetrons. Permanent magnets, electromagnets, or a combination of both have been used. The magnets can be set to fit circular or rectangular planar targets, or cylindrical targets. In a study carried out by Kirov et al. [47] the importance of the magnetic field lines being parallel to the cathode was observed. They used an electromagnet in a planar magnetron system to compare the discharge current-voltage relationship of the two different central magnetic pole designs. The first design consisted of the central pole piece extending up to the back of the cathode. The central pole piece in the second design was extended 15 mm past the cathode surface. It was found that for the same coil current the discharge current in the second case was about one order of magnitude higher than the first while at half the voltage and at much lower gas pressures. With a cathode voltage of 700 volts, argon pressure of 6.67×10^{-2} Pa the discharge current was 700 ma for the second design

while with a cathode voltage of 700 volts, argon pressure of 1.36 Pa the discharge current was 120 ma for the first design. The improvement caused by the extended pole piece is due to the magnetic field lines becoming more parallel to the cathode surface. It was also found that as the cathode diameter increased, the differences between the characteristics of the two center pole types decreases.

Because of the high power dissipations at the cathode surface, the cooling of the cathode is very critical. To obtain the required cooling rate the target is bonded to a backing plate [48] which forms one wall of the cooling chamber. The coolant used most commonly is water. The flow rates required are relatively high.

By operating the plasmas with a ring anode which is close to the target, such that the ring anode is at a positive potential relative to the substrate, the distribution of the electron current between the substrate and anode can be altered. Schiller et al. [49] found that by keeping both substrate and the anode at the same potential, an electron current of the same order of magnitude as the discharge current flows to the substrate. Even a low potential difference of 35 V between the anode and substrate causes nearly all the electrons to drift to the anode, which reduces the heating of the substrate.

Because of the extremely high ion current density on the target, the sputtering rates are very high. For the ring-gap

plasmatron [49] using a power of 5KW, and a chamber pressure of 0.4 Pa, the sputtering rates of copper and aluminum are 0.7 grams per minute and 0.1 grams per minute, respectively. The deposition rates at a substrate-target distance of 50 mm is 2.5 microns per minute for copper and 1.1 microns per minute for aluminum. Similar coating rates have been obtained by using the cylindrical magnetron system.

In conventional dc sputtering, secondary electrons emitted by the cathode are accelerated across the dark space and, unless the substrate is shielded or negatively biased, will bombard the substrate with almost full energy of the cathode potential. Of the estimated 40 percent of the applied power dissipated at the substrate, almost all of it is due to the secondary electrons [50]. In magnetron sputtering the secondary electrons are accelerated by the potential difference between the cathode and the plasma, but they are influenced by the magnetic field and become trapped until the energy level is reduced by ionization collisions [17,18,46]. Some electrons do escape in the planar magnetron system by following magnetic field lines emerging from the cathode (usually in the central regions). Since the majority of the electrons are trapped, the substrate heating is reduced, but due to the high deposition rates the heat of condensation can cause substrate heating.

According to Clarke [10], when using the dc magnetron system for reactive sputtering there are three design

parameters which have to be considered. First, the plasma has to be confined to the total exposed area of the cathode surface. When areas of the cathode are not sputtered, there will be a build up on the cathode of the reactive sputtered material, some of which may be dielectric. These dielectric areas can charge up and discharge to the cathode surface producing arcs. This type of arcing was also observed by Chapin [46], who called them "racetrack" arcs and "looping" arcs.

The second design requirement is the high power density to the cathode surface. High current density is necessary to erode the target material faster than it can react with the reactive gas. High voltage is preferred because as voltage increases, sputtering yield increases.

The final important design aspect is effective cooling of the target. Not only is it due to the high power dissipated at the cathode but also because temperature of the target can be very significant to the adsorption action at the target.

There are two very excellent reviews on magnetron sputtering systems in the recent literature. Thorton [17] has discussed the basic physics and application to cylindrical magnetrons. Waits [51] emphasized the design, performance and application of the planar magnetron sputtering systems.

CHAPTER III

EXPERIMENTAL EQUIPMENT AND PROCEDURE

Sputtering System

The sputtering system utilized in the current program consists of four different sub-systems: (1) the vacuum system, (2) two power supplies, (3) the gas supply system, and (4) the magnetron system. Each sub-system is very important for the proper sputtering operation. The design is as simple as possible, yet is versatile enough to allow for the testing of many different parameters such as substrate heating or biased sputtering. The system could easily be modified for commercial batch type use (see Figure 4).

The vacuum system has two significant purposes. First it is to limit the amount of impurities in the sputtering environment by the initial evacuation of the sputtering chamber. The second function is to maintain the sputtering chamber at the operating pressure. The components of the vacuum system used for this work consists of a vacuum chamber, diffusion pump, mechanical pump, and assorted valves. The chamber is a 305 mm (12 in) diameter by 305 mm high pyrex glass cylinder with a top plate which supports the magnetron system, gas feed inlets, and a vacuum gauge. The vacuum chamber rests on a stainless steel base plate which contains

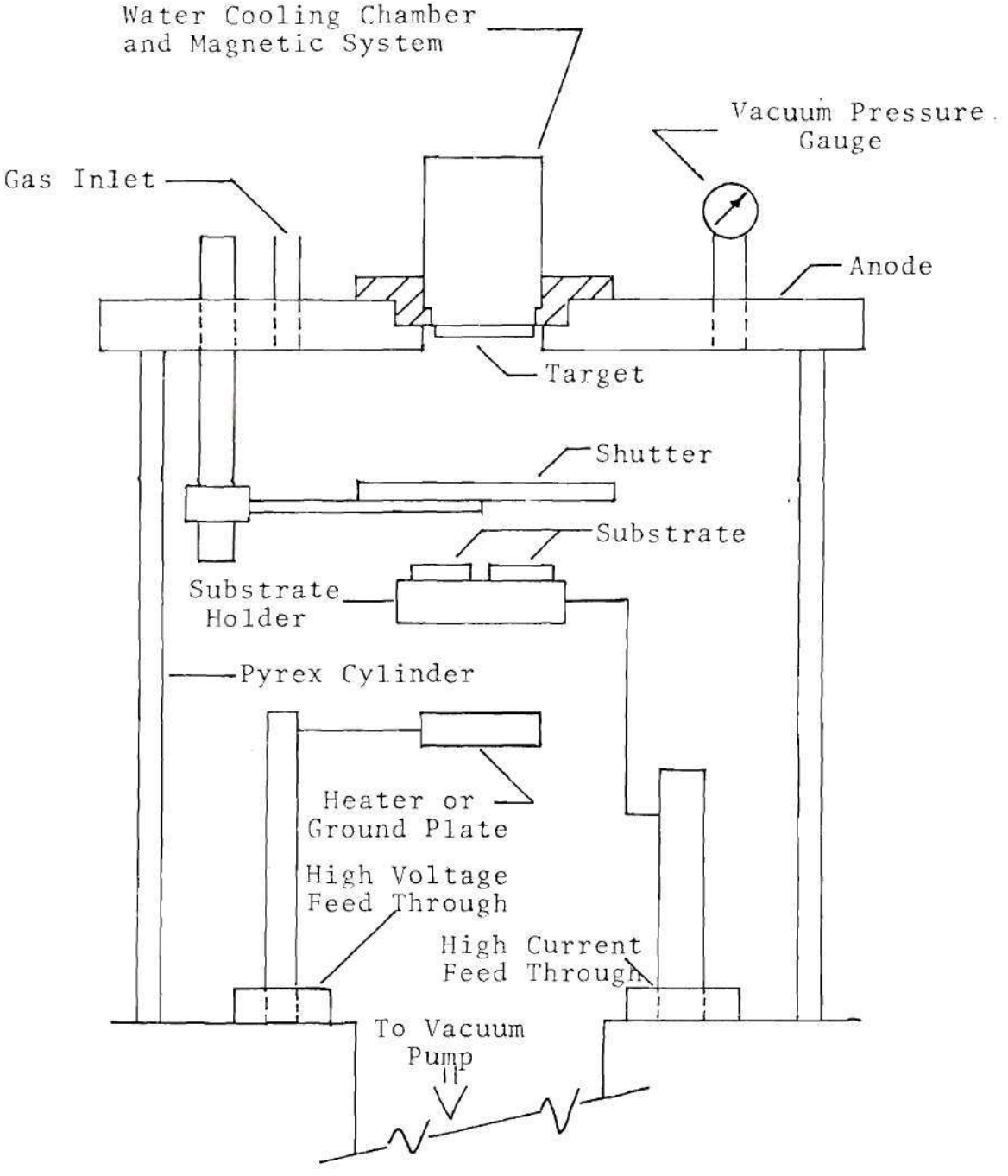

Figure 4. Schematic Diagram of a Magnetron Sputtering System

two high voltage feed throughs and two high current feed throughs and is connected to the pumping system. The pumping system is a unit marketed by Consolidated Vacuum Corporation (CVC). It contains a 102 mm (4 in) diffusion pump (CVC Model PMC-4B) and a 160 liter per minute (5.6 CFM) mechanical pump (Welch Type 1402B) connected by a valve arrangement to allow for the proper evacuation of the chamber. The pressure in the vacuum chamber and pumping system is monitored by thermocouple vacuum gauges (CVC GTC-004 and Hastings DV-5M).

Two power supplies are used. The first is a CVC glow discharge power supply type LC-031 which is a high reactance, variable voltage, dc power supply. It is rated at 300 ma continuous duty or 500 ma at 50% duty cycle and has an output voltage of 5 KV. The other power supply is a Hipotronics dc power supply model 801-2500 with voltage and current capabilities of 1000 volts and 2500 ma. It is a low reactance power supply equiped with a Thyrister overload (1 millisecond sense, 1 cycle trip) protection.

The power supply used for dc sputtering must be designed to prevent the possibility of a transition of the discharge from that of an abnormal glow into that of an arc. This requirement is even of greater importance for the power supply used for reactive sputtering. Several methods are available for achieving this requirement. One solution is to use a large ballast resistor in series with the discharge, but the resistor may consume 30 percent or more of the output

power. Another technique is to use a high reactance transformer in the power supply which limits the output current when it is completely short-circuited. The high reactance transformer has a high efficiency when compared to that of a supply using a limiting resistor. The final method is to place a saturable reactor in series with the primary lead of the high voltage transformer. This method has an efficiency comparable to that of the high reactance transformer.

The CVC power supply is equipped with a high reactance transformer and meets the design requirements. The Hipotronics power supply is not equipped with any of the design requirements so a 1.5 henry choke was placed in series with the high voltage lead. Both power supplies proved to be satisfactory and were able to recover immediately after any arcing which may have occured during sputtering.

The gas supply system is responsible for transporting, purifying, drying, and metering gas from the gas tank to the vacuum chamber (see Figure 5). The gases used for this work were argon and nitrogen. The argon was a high purity grade and the nitrogen was an extra-dry grade. The gas was dispensed out of the tank by a regulator, then the gas flowed through a gas purifying column into a flowmeter and to a flow controlling needle valve (Grinville-Phillips Co., Series 203). After flowing through the needle valve the gases are mixed (when using both gases), then pass through an oxygen trap and into the vacuum chamber. The flow meter used for the

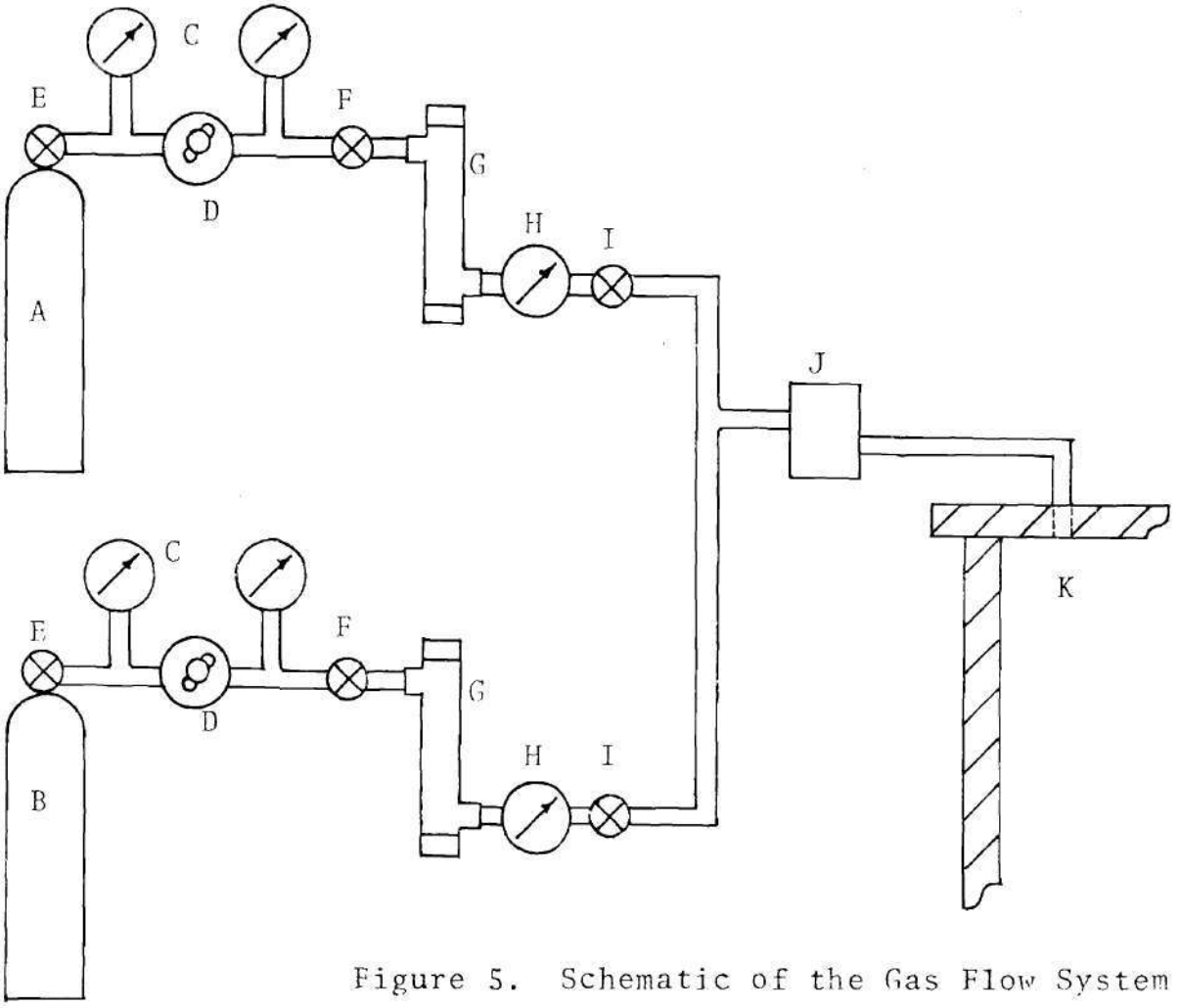

A--argon gas

B--nitrogen gas

C--pressure gauges, 0-300 psig

D--regulator

E--high pressure valve

F--valve

G--gas purifying column

H--flow meter

I--needle flow control valve

J--oxygen trap

K--vacuum chamber

Figure 5. Schematic of the Gas Flow System

argon was a Tylan, Model FM-360 mass flowmeter, calibrated for argon of flows of 0 to 11.5 sccm. The flow meter used for the nitrogen was a rotometer (Croydon, R398426) capable of measuring flows of 0 to 50 sccm.

The magnetron system required major development work. It contains the cathode, anode, substrate holder, shutter, and a magnetic field. The anode is the cylindrical top plate on the vacuum chamber. The water-cooled cathode sits in the center of the anode separated from the latter by insulation. The cathode is a plate 1.5 mm thick of commercial grade titanium. A magnetic system rests flush with the back of the cathode. The substrate holder is connected to a high voltage feed-through so that the substrate could be sputter cleaned prior to film deposition or kept at a biased potential during film deposition. The stage lies parallel 52 mm below the cathode. The shutter must be height adjustable so that it can be placed near the cathode or the substrate. The shutter is used to keep the cathode from being coated with impurities while sputter cleaning the substrate and visa-versa.

Sputtering Procedure

The procedure used for sputtering is a sequential step by step process. Before the substrate is placed in the chamber it is cleaned ultrasonically in an acetone bath, then rinsed with alcohol and finally dried with an air blower. Once the substrate is in the chamber and the chamber sealed off from the environment, the mechanical pump is used to

evacuate the chamber down to 7 Pa. The mechanical pump is closed off and argon leaked into the chamber until the pressure is up to 270 Pa. The mechanical pump again evacuates the chamber to 7 Pa. The diffusion pump is then used to bring the chamber pressure to 0.13 Pa. Argon is leaked into the chamber (at 5 sccm) and the pressure is increased to 3.3 Pa by using a throttle valve between the chamber and diffusion pump. The shutter is placed between the cathode and substrate near the cathode. A negative potential (-2000 V) is applied to the substrate which is sputter cleaned for 20 minutes. The substrate is then grounded and the shutter brought near the substrate. The pressure is adjusted to 0.4 Pa and the target becomes the cathode and is sputter cleaned. For non-reactive sputtering the shutter is removed, but for reactive sputtering reactive gas (e.g. nitrogen) is introduced and after stability is obtained the shutter is removed. After the coating is completed the substrates are allowed to cool in the reactive environment of 27 to 67 Pa pressure for 15 minutes.

Prior to the installation of the Hipotronics power supply, the deposition rates and film thickness uniformity for titanium at 200 ma, 300 ma, and 400 ma discharge current and cathode-substrate distance of 50 mm was determined. The procedure used for this is as follows. A glass slide is placed on the substrate holder and is

covered with an aluminum sheet which has 3.18 mm diameter holes spaced 12.7 mm radially outwards. For each discharge current the sputtering durations are 1000, 1500, and 2000 sec. After deposition the aluminum sheet is removed and the glass slide will have circular deposites of titanium films corresponding to the holes in the aluminum (see Figure 6). The thicknesses of these films are measured with a surface roughness measuring device (Bendix Group XV proficorder-microcorder system). The thickness uniformity can be observed from the thickness measurements directly. The deposition rates can then be found by plotting the thickness of the films against time for each corresponding set of deposits. The slope of the line going through zero and the plotted points is the deposition rate.

When heating the substrate was undertaken, an additional step was inserted into the sputtering procedure. The substrate was heated by radiant heat from a 50 mm disc heater placed 20 mm below the substrate holder. A thermocouple was located between the substrate holder and the heater near the substrate holder. The heater was turned on once the chamber was at 1 Pa pressure and turned off when the thermocouple read 130°C. The substrate was then sputter cleaned according to the procedure outlined above.

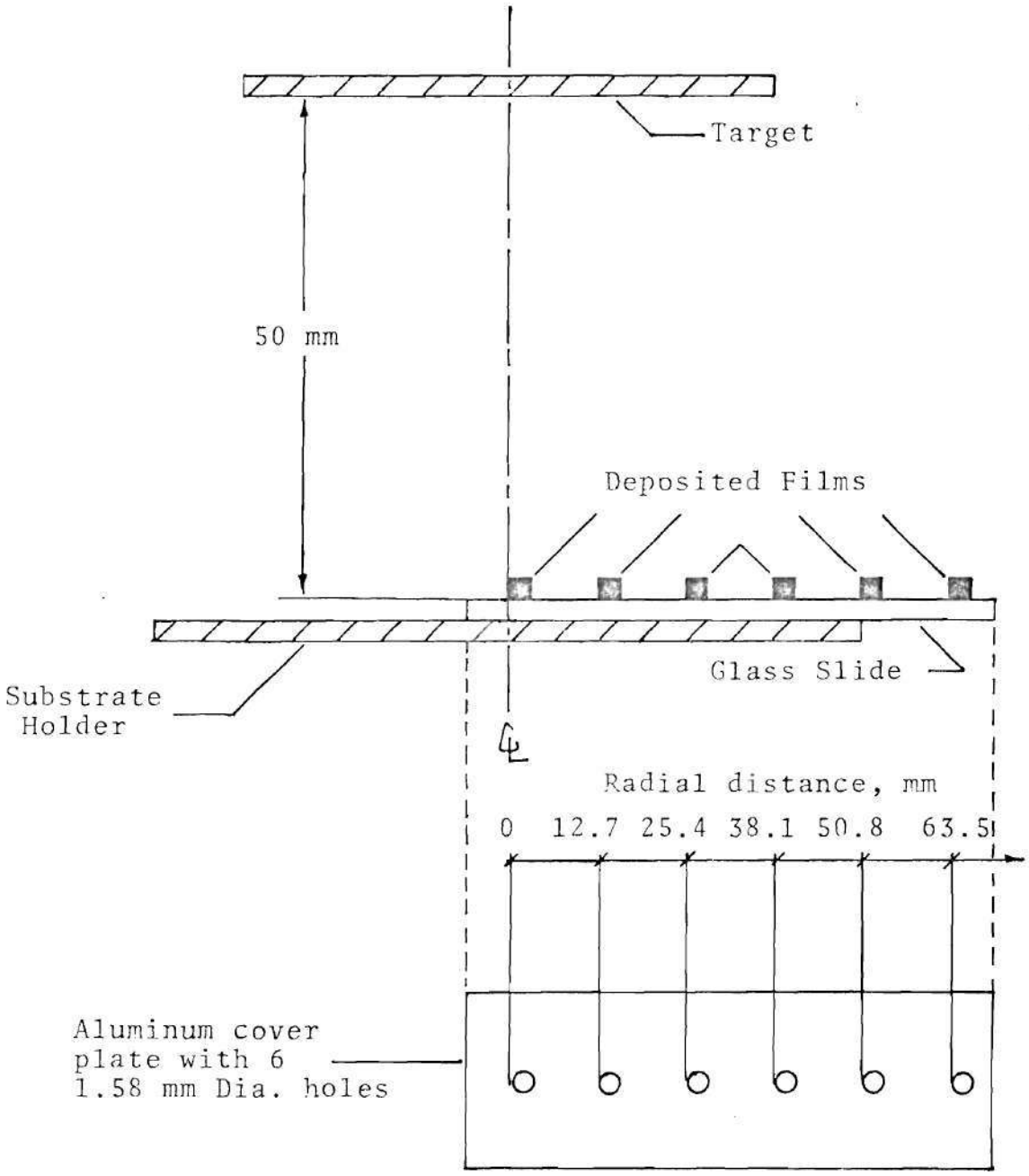

Figure 6. Substrate Position for Determining Coating Rates and Film Deposition Uniformity

Film Composition

The technique used to determine the chemical composition of the sputtered films is that of x-ray diffraction. The specimen are scanned through a 2θ of 30 to 70 degrees in filtered Ca Kα (K-alpha) radiation. This 2θ scan range includes the diffraction peaks of Ti(101) at 40.15°, TiC (111) at 35.2°, TiC (220) at 59.7°, TiN (200) at 42.30°, and TiC (113) at 67.8°.

Machining Test Technique

The machine used for the turning tests was a Springfield lathe driven by a 10 hp motor. The speed is controlled by a gear drive system.

To compare the coated tools to the uncoated tools for resistance to crater formation a simple turning test was developed. The depth of cut and feed are kept constant at 1.5 mm (0.06 in) and 0.135 mm per revolution (0.0053 in/rev) respectively. The rotational speed is constant, so as the diameter changes the surface speed changes. This means that after running tests over the length of the bar, the machining condition changes. To account for this difficulty two things are done. First, the time is varied so that the total surface length machined is constant:

$$\text{Surface Length} = C_a \times \text{time} = 460 \text{ meters}$$

where C_a is the average surface speed. The cutting speeds varied from 107.4 meter per minute to 87.0 meters per minute. Second, the length of the machined bar is long enough for three tests to be run at the same diameter, so one uncoated tool is tested at each diameter.

The material machined was AISI 1045 steel (HRC 19). Its composition is given in Appendix A. The base cutting tool is a tungsten carbide insert grade 883-SNG432 provided by the G.E. carboloy group. The tungsten carbide tool is used because a very distinct crater is formed rapidly on the rake face of the tool while machining steel. The actual wear mechanism which causes this crater formation is believed to be one of two conflicting ideas. Ramalingam and Faulring [52] and Byrd and Ferguson [53] provide strong evidence suggesting that the wear process is due to abrasive particles in the work piece. Liquification of the cobalt binder phase has been observed to occur at 1325°C by Williams [54]. This temperature is indeed reached in a thin layer of the tool at the tool-chip interface at high cutting speeds [55]. Therefore the tool is very soft in this layer and the aluminum oxide or other inclusions in the steel can "plow" the tool material away. N. Cook and others [56,57] believe the wear is due to the diffusion of the carbides at the high temperature reached at the tool-chip interface. Irrespective of the wear mechanism the TiN coating should function as a protective

coating either by presenting a temperature resistant, high hardness material for abrasive resistance or by acting as a diffusion barrier.

After the turning tests were completed the crater depth was measured with a profilometer which was used previously for measuring film thickness. The depth of the crater was measured six to eight times over the tool-work piece contact length. The deepest point measured is used as the depth of the crater (see Appendix B).

CHAPTER IV

EXPERIMENTAL RESULTS AND DISCUSSION

Deposition Uniformity and Coating Rates

One of the important requirements of any coating system is the deposition of a uniformly thick film onto the substrate. This is desirable because the properties of the coating will be more uniform. In sputtering systems the uniformity of the deposits is controlled by the cathode-substrate spacing, size of the cathode, geometry of the cathode-substrate arrangement, and relative motion between the substrate and cathode.

The deposition uniformity of the sputtering system used in this study is shown in Figure 7. The decrease in the film thickness in the radial direction is due to the small size of the target. According to Waits [51] the sputtering thickness distribution usually agrees with calculations based on the cosine emission of sputtered material from the erosion area [22]. Chapin [46] and Schiller [18] have obtained uniformly distributed films for a radial distance of over 70 mm from the center axis at a cathode-substrate distance of 50 to 60 mm by using a similar magnetron system but with a larger cathode diameter (approximately 150 mm).

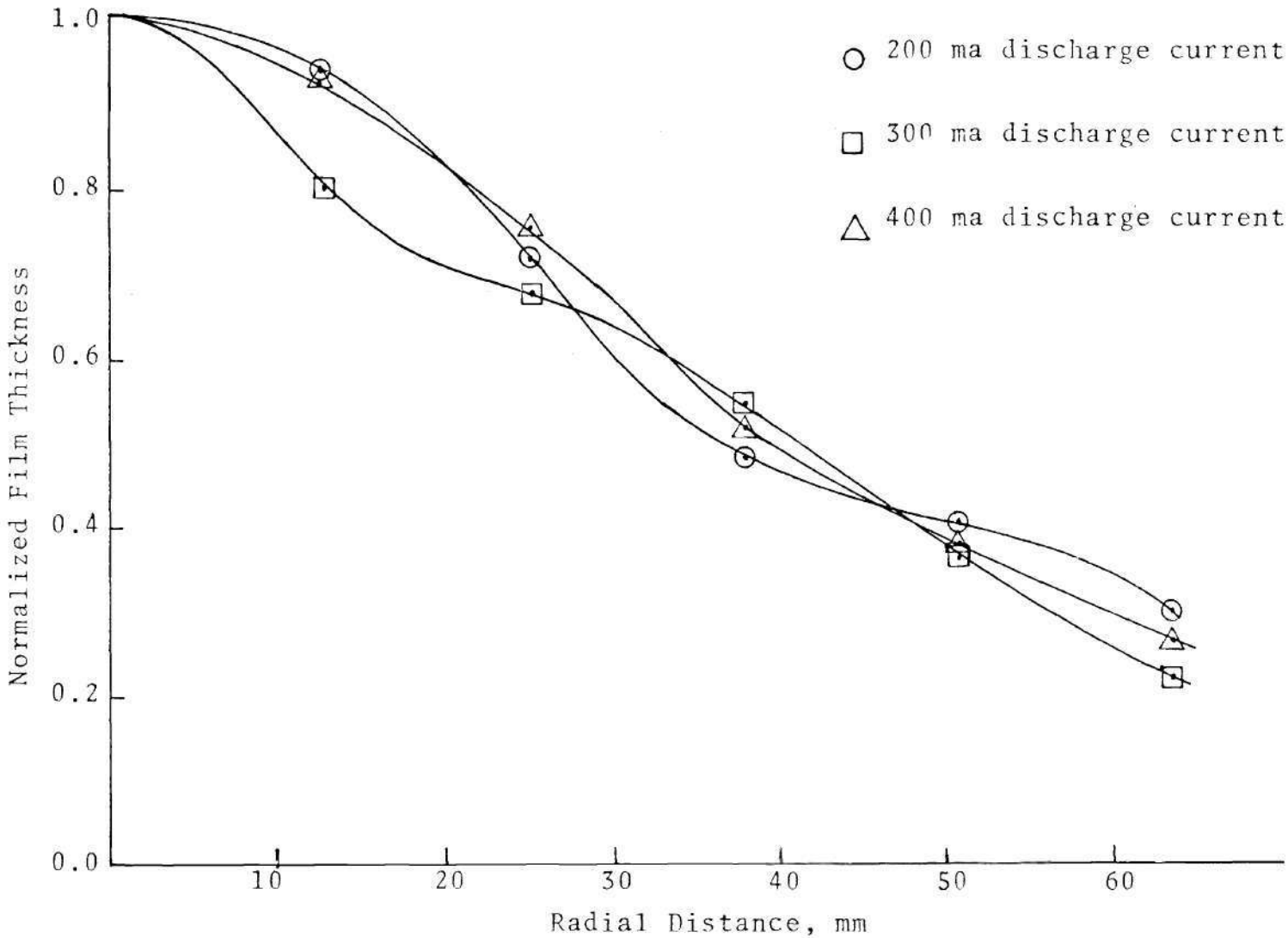

Figure 7. Radial Film Thickness Distribution in the Magnetron Sputtering System

The maximum deposition rate measured for titanium in an argon environment for the system used in this study was 0.09 microns per minute at 400 ma x 600 v which provides an average power density of 12 W/cm^2 (see Figures 8-10). The deposition rate should be proportional to the power density with constant pressure in the range of pressures current and voltage used in this study. The maximum power density obtained was 85 W/cm^2 which should provide a deposition rate of 0.64 microns per minute. By using a larger target area the deposition rates would be increased further.

Target Cooling

Originally the target was held against the backing plate, which was water cooled, by clips. This system appeared to be satisfactory while operating the system at 200 to 400 ma in an argon environment. When sputtering at higher current densities, the target became red hot (temperature >600°C). The titanium target became hot enough to recrystalize and warp and on one occasion a copper target heated up sufficiently to become partially melted (temperature >1080°C) (see Figure 11). While reactive sputtering the arcing problem became uncontrollable. As the titanium target became hotter it began to act as a getter pump by adsorbing nitrogen, in so doing dielectric material formed on the target which charged up and discharged

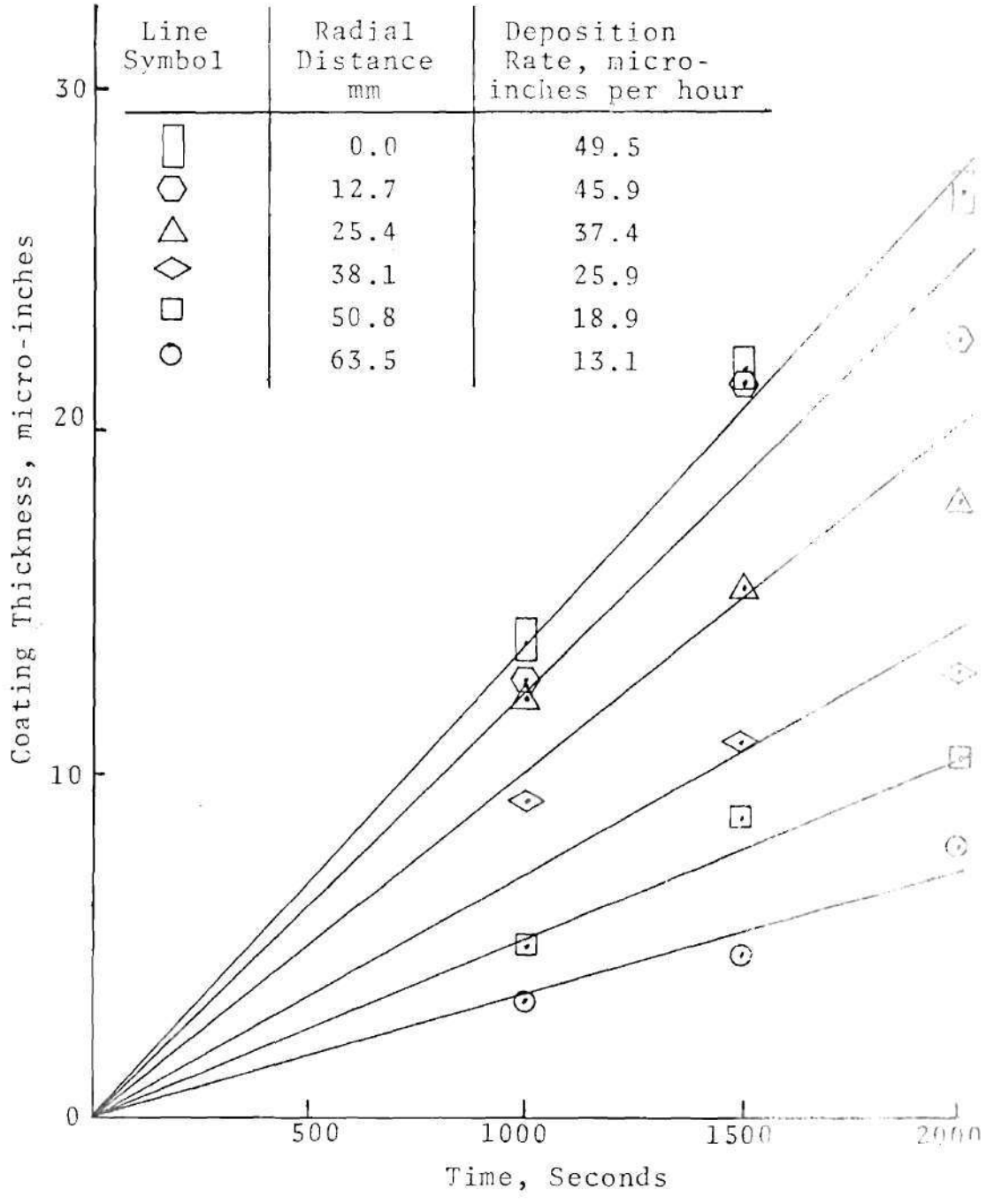

Figure 8. Film Thickness as a Function of Coating Time for Discharge Current of 200 Milliamps. Slope of lines are corresponding deposition rates. Sputtering at 200 ma X 600 volts cathode potential. Separation distance between cathode and substrate is 50 mm. Radial distance as noted.

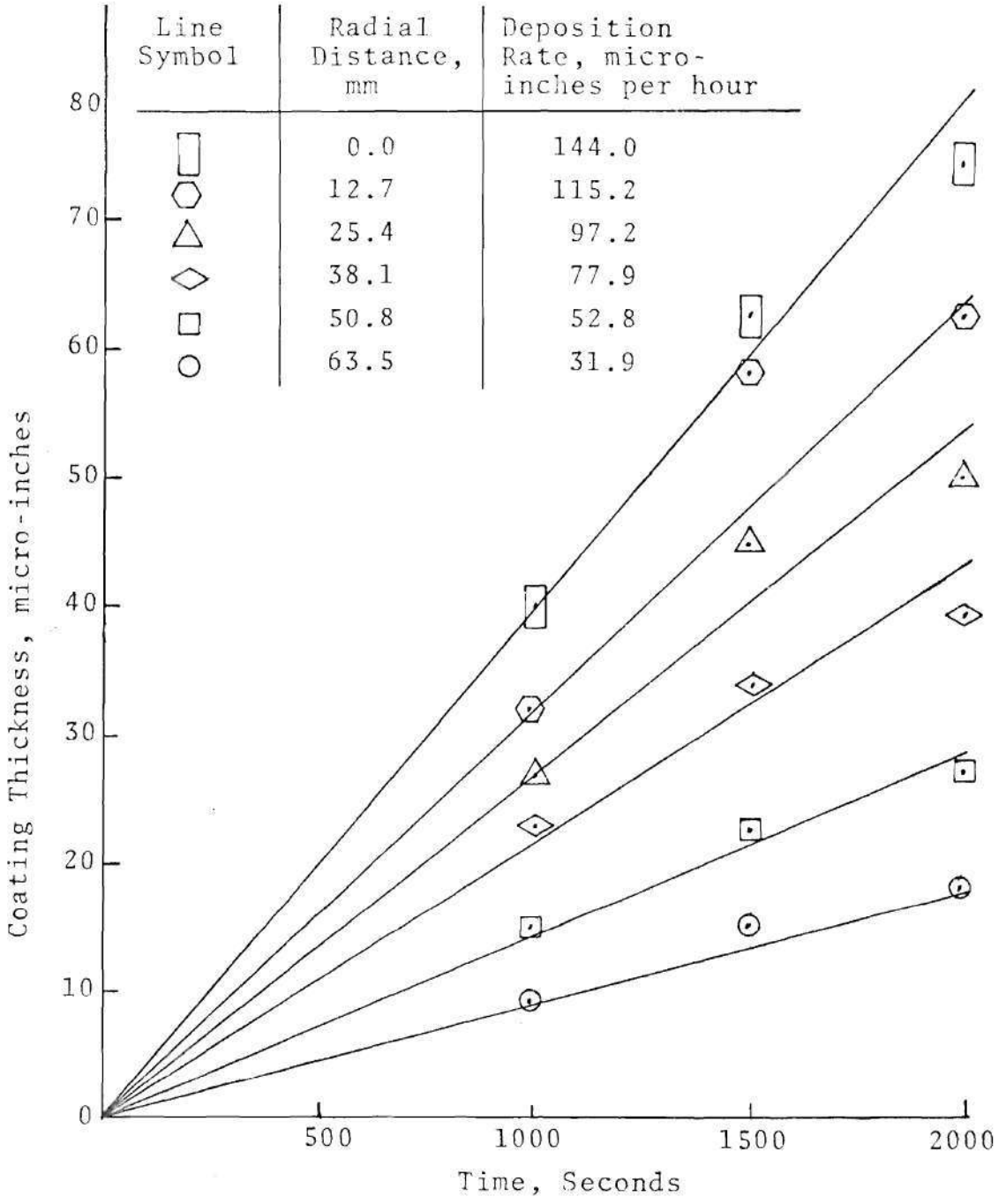

Figure 9. Film Thickness as a Function of Coating Time for Discharge Current of 300 Milliamps. Slope of lines are corresponding deposition rates. Sputtering at 300 ma X 600 volts cathode potential. Separation distance between cathode and substrate is 50 mm. Radial distance as noted.

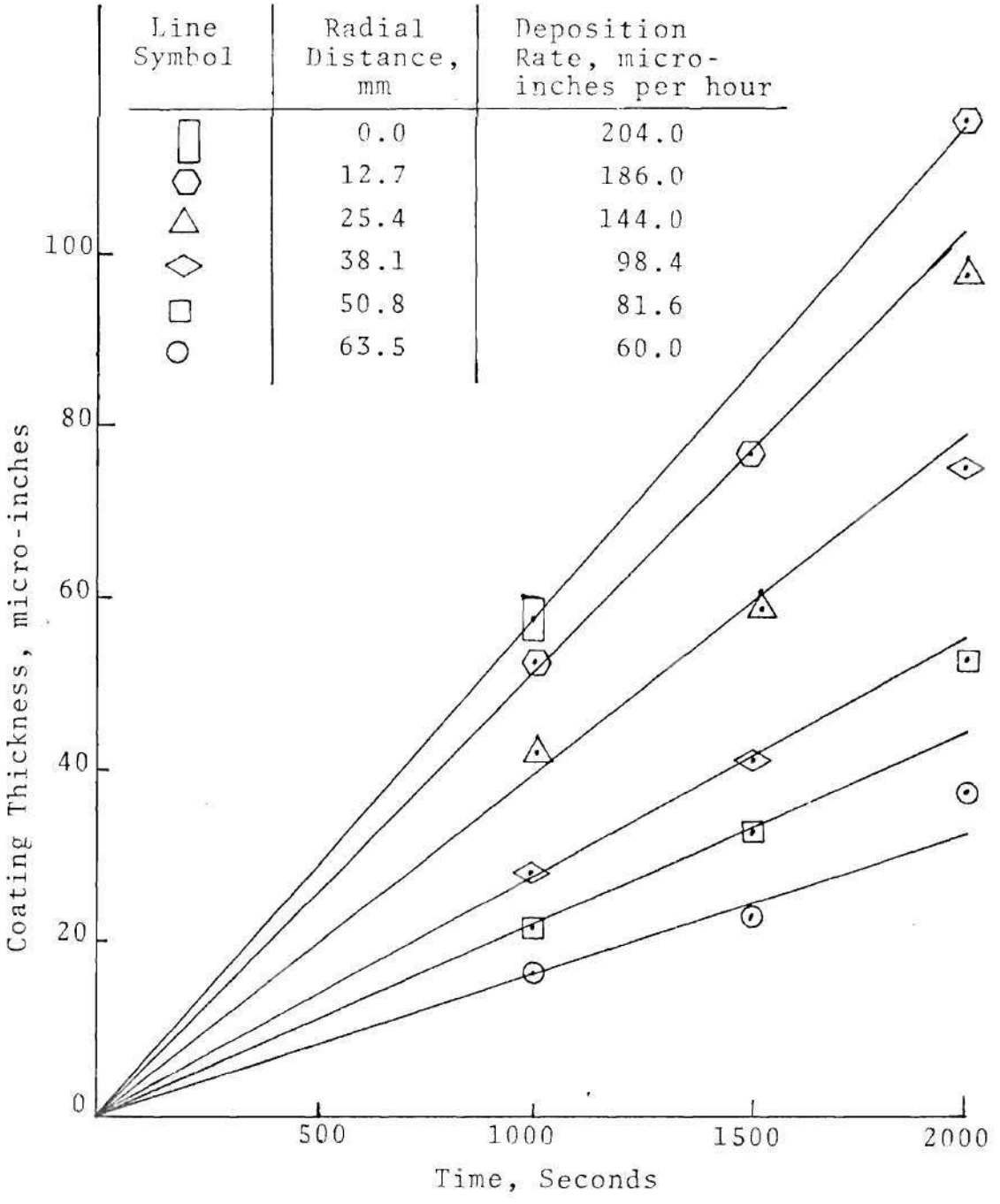

Figure 10. Film Thickness as a Function of Coating Time for Discharge Current of 400 Milliamps. Slope of lines are corresponding deposition rates. Sputtering at 400 ma X 600 volts cathode potential. Separation distance between cathode and substrate is 50 mm. Radial distance as noted.

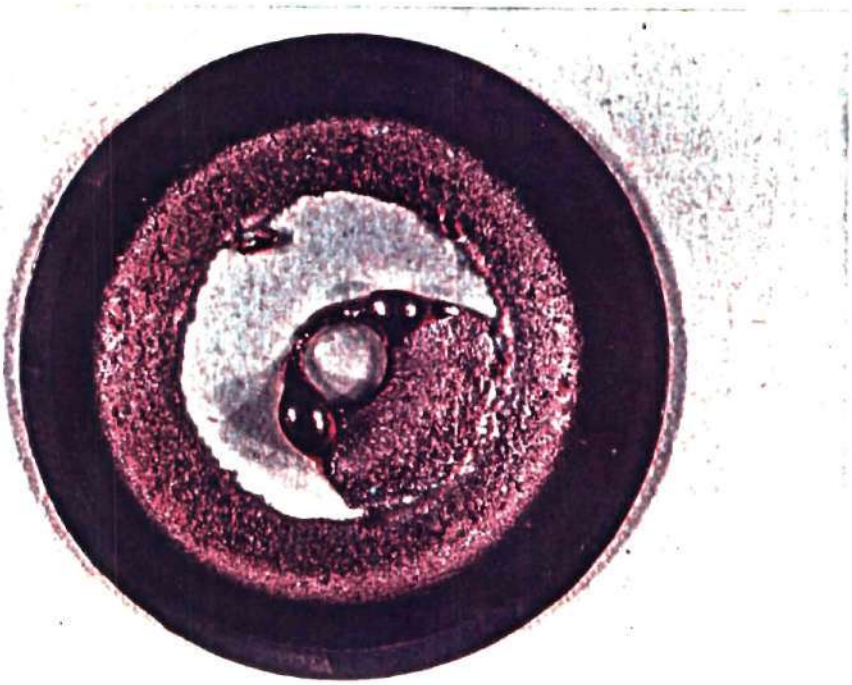

Figure 11. Copper Target Sputtered at 750 ma X 700 Volts. Target was clipped to water cooled backing plate, but still heated to melting temperature.

as an arc. A survey of the literature showed that the cooling of the target is a serious problem [48]. The solution developed to increase target cooling was to nickel plate the titanium target and then use lead-tin solder to join the target to the backing plate. This technique improved the system sufficiently so that sputtering could be carried out at a power of 2000 ma x 870 volts on a 5 cm diameter target (85 W/cm^2) for over 30 minutes without excess target heating.

Parameters Adjusted for Reactive Sputtering

There are several quick methods which can be used to approximate film composition and adhesion properties when determining the best conditions for obtaining TiN by reactive sputtering. The first method is the observation of the film color. It has been observed that TiN is a copper-bronze [58] or gold color [10] and TiN_x ($x > 1$) films are a deep rose to deep blue color [10]. A simple adhesion test beyond the observation of peeling or flaking is the scotch tape test. The tape is applied to the film and then rapidly removed. If the film remains on the substrate the adhesion is considered to be strong enough to withstand the test [59].

The conditions which are varied are substrate heating, flow rate of nitrogen, total pressure, bias potential applied to the substrate, and power density applied to the

target. The heating of the substrate was abandoned because the color of the deposits did not have any improvement over substrates which were coated under the same conditions except for substrate heating and because of poor adhesion of the film when substrate heating was used.

Total pressure was varied because of two purposes. For a constant discharge current the voltage increases as the pressure decreases. Clarke [10] demonstrated that the reduced field, E* can be correlated to the formation of TiN and that for the S-gun magnetron design, E* was between 7.5 and 8.5. By lowering the pressure, E* is increased due to both the increased voltage and decreased pressure. For the system used in this work it was observed that for an E* less than four (4) the film color was a deep blue to a light purple and for E* between 4 and 6 the film color was pinkish to a copper-bronze color. The color of the films tested in the machining tests were pinkish to copper bronze in color and the corresponding reduced fields were between 4 and 6.

According to Clarke [10] the percentage of nitrogen has no effect on the formation of TiN other than the fact that enough nitrogen must be available for the adsorption of nitrogen to occur. He shows that for an E* of 7.5 to 8.5, TiN will form at the substrate for nitrogen percentages of 50 to 75. The outcome of this study seems to agree with Clarke's findings, but nothing conclusive can be said from

the present study in this area. There are some very pronounced effects due to the nitrogen concentration on the sputtering rate as well as the voltage-current characteristics of the system. When sputtering with a chamber pressure of 2 Pa, 75% nitrogen, and 525 volts applied to the cathode, the discharge current is 300 ma, but for the same chamber pressure and cathode potential and 33% nitrogen the discharge current is 500 ma. From visual observation it appeared that as the nitrogen concentration increased the sputtering rate decreases for similar current densities. From the studies of Almen and Bruce [33] it was observed that the sputtering yields were maximum for noble gas ions and almost zero for ions of reactive gases such as nitrogen. The first ionization energies of argon and nitrogen are 15.755 and 14.54 eV [60], respectively. For an environment of 50% nitrogen and 50% argon, of the ions formed 50% could be nitrogen ions,[3] so 50% of the ionization collisions cause almost no atomic ejection of target material and the sputtering rate is reduced by 50%. The voltage-current characteristics are affected because as the percent nitrogen increases the percent of inefficient collisions increase also. As the atomic ejection rate decreases so does the ejection of secondary electrons which causes the ionization of the gases.

The effect of biased sputtering was not fully studied.

[3]Assuming that the size of the nitrogen and argon species are the same size.

Schiller et al. [49] showed that the discharge current can be shifted from the substrate to the ring anode which decreases substrate heating. This effect was not studied in this work, but the substrate was never observed to be hot (temperature <200°C). The color and shape of the glow discharge was effected by biased sputtering. When reactive sputtering a biased potential (-46 volts) applied to the substrate helped stabilize the discharge.

Distribution of Ti_xN_y-Interpretation of the Reduced Field

It was observed from deposits from reactive sputtering on glass slides that there was a radial color change. Also it was observed that the color of the plasma discharge changed colors when the reactive gas was admitted into the system except for the color of the discharge at the target surface. These two observations can be used to explain the importance of the cathode-substrate distance in the formation of TiN as shown in Figure 12. In the calculation of the reduced field the cathode-substrate spacing (cathode-anode spacing) is in the denominator. Therefore for short cathode substrate spacing, E* is large which corresponds to the Ti + TiN zone. For medium cathode-substrate spacing, E* is medium corresponding to the TiN zone. For large cathode-substrate spacings, E* is small corresponding to the TiN + TiN_2 zone.

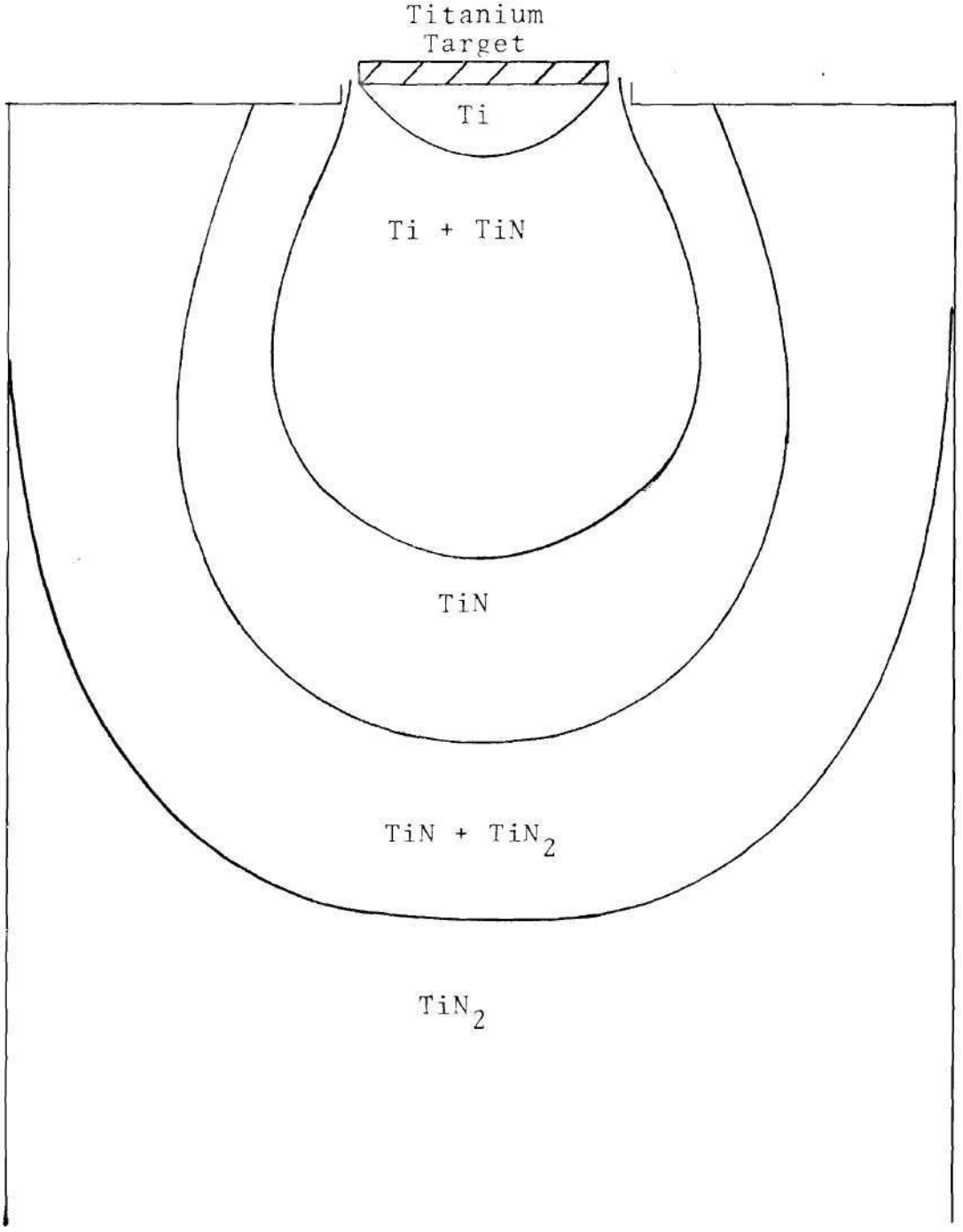

Figure 12. Schematic Illustration of the Distribution of Nitrogen Reaction with Sputtered Titanium

Coating Compositional Analysis

The film deposition parameters for the coating of the Tungsten Carbide tools by the Magnetron Reactive Sputtering technique are given in Table 2. From these coating conditions a list of compounds which are expected to be formed on the substrate can be developed. A summary of the expected compounds along with their peak location for X-ray Diffraction analysis is presented in Table 3. Titanium is expected to form because it is possible that not all of the sputtered Titanium reacted with the nitrogen. TiN is expected because the sputtering does occur in the presence of the reactive gas nitrogen. TiC could be present because of carbon atoms being available from the back-streaming of diffusion oil or from the Tungsten Carbide substrate. Since the coating thickness is small, Tungsten Carbide in addition to Cobalt which are both present in the substrate material can be expected to be detected. The expected 'fine grain size' in the coating would produce broad and diffuse peaks in the diffractometer traces. Of the compounds listed in Table 3, Column 5 shows the strongest reflection from each of the materials. Column 6, Table 3, lists the relative intensities of appreciable magnitude that are possible for the materials listed.

The tools analyzed by X-Ray Diffraction were S2, S4, and S6. The summary of the x-ray analysis for the coated sampels S2, S4, and S6, are presented in Tables 4, 5, and 6,

Table 2. Film Deposition Parameters for the Coating on the Tungsten Carbide Tools Evaluated in Machining Tests

Tool	Discharge Current	Voltage	Cathode Substrate Spacing	Partial Pressure Nitrogen	Radial Spacing	Bias Voltage
S2	600 ma	550	50 mm	0.223 Pa	12.7 mm	0
S3	600 ma	550	50 mm	0.223 Pa	25.4 mm	0
S4	600 ma	550	50 mm	0.223 Pa	38.1 mm	0
S6	1000 ma	600	50 mm	0.277 Pa	12.7 mm	-46
S7	1000 ma	600	50 mm	0.277 Pa	25.4 mm	-46
S8	1000 ma	600	50 mm	0.277 Pa	38.1 mm	-46

Table 3. Summary of the Peaks Expected in the X-Ray Diffraction Analysis of the Samples. Cu-Kα Radiation: Wave Length = 1.542 Å.

No.	2θ	d	hkl	Compound	Intense Line	Rel Intensity
1	31.58	2.83	001	WC		WC-70
2	35.05	2.557	010	Ti		Ti-30
3	35.72	2.51	111	TiC		TiC-80
4	35.73	2.51	100	WC		WC-80
5	36.79	2.44	111	TiN		TiN-75
6	38.38	2.342	002	Ti		Ti-26
7	40.13	2.244	011	Ti	Ti-100	Ti-100
8	41.38	2.179	200	TiC	TiC-100	TiC-100
9	41.66	2.165	100	Co		
10	42.59	2.12	200	TiN	TiN-100	TiN-100
11	44.65	2.027	110	Fe	Fe-100	Fe-100
12	44.74	2.023	002	Co		Co-60
13	47.55	1.910	101	Co	Co-100	Co-100
14	48.63	1.87	101	WC	WC-100	WC-100
15	52.98	1.726	012	Ti		
16	60.21	1.535	220	TiC		TiC-50
17	61.95	1.496	220	TiN		TiN-55
18	62.70	1.48	102	Co		
19	62.93	1.475	110	Ti		WC-60
20	64.05	1.452	110	WC		
21	64.99	1.433	200	Fe		WC-50
22	65.62	1.421	002	WC		
23	70.63	1.332	103	Ti		

Table 4. Summary of the X-Ray Diffraction Analysis of Coated Sample S2

Peaks Observed at 2θ	Peak Height Above Background	Compound Identified	Plane hkl	Line Character
31.6	130	WC	001	sharp
35.8	450	WC	100	sharp
36.8	Overlapping peak	TiN	111	Overlaps WC 100
42.6	50	TiN	200	diffuse
48.6	500	WC	101	sharp
61.9	40	TiN	220	diffuse
64.1	110	WC	110	sharp
65.6	50	WC	002	sharp

Table 5. Summary of the X-Ray Diffraction Analysis of Coated Sample S4

Peaks Observed at 2θ	Peak Height Above Background	Compound Identified	Plane hkl	Line Character
31.6	230	WC	001	sharp
35.8	710	WC + TiC(?)	100 111	sharp
36.8	50	TiN	111	diffuse
37.8	30	Unidentified possibly an oxide		diffuse
42.6	110	TiN	200	diffuse
48.6	out of scale	WC	101	sharp
61.9	20	TiN	220	diffuse
64.1	140	WC	110	sharp
65.6	60	WC	002	sharp

Table 6. Summary of the X-Ray Diffraction Analysis of Coated Sample S6

Peaks Observed at 2θ	Peak Height Above Background	Compound Identified	Plane hkl	Line Character
31.6	70	WC	001	sharp
35.8	240	WC	100	sharp
36.5	140	TiC:TiN	111	diffuse
38.38	110	Ti	002	sharp
42.6	80	TiN	200	diffuse
48.6	300	WC	101	sharp
61.2	80	TiC:TiN	220	diffuse
64.1	70	WC	110	sharp
65.6	25	WC	002	sharp

respectively. In the x-ray analysis system used, a systematic error of 0.2° was observed in all peaks. The data shown is corrected for the instrument error.

For sample S2, the full width at half maximum of the TiN (200) peak is 1.6°. All the diffuse peaks of TiN are broad indicative of fine grain size in the coating. The TiN peak from the 111 reflection overlaps the WC 100 peak and is observed as an asymmetric tail of WC 100 peak. The diffractometer traces obtained are substantially comparable to that obtained from sample S4. The relative intensities are, however, lower than those in sample S4. The difference is attributed to the formation of a smaller thickness film. No clear-cut evidence is observed indicative to the formation of TiC in the coating process. The principal TiC peak at 41.38° from the 200 reflection of TiC is not observed. The observed data implies that fine grained films of TiN have been produced.

The full width at half maximum of the TiN peaks in sample S4 are large and comparable to those in sample S2. The relative intensities observed for the TiN peaks are in the same order as would be expected in pure TiN compounds. We may therefore infer that while there may be a texture, it is most likely not very strong. At the 35.8° peak, WC and TiC peaks may be overlapping. The principal peak of TiC at 41.38° was not observed, so it is safe to conclude that the coating is probably pure TiN.

The peaks observed at a 2θ of 36.5° and 61.2° in

sample S6 were observed approximately between the expected TiC and TiN peaks. The unique single peak and the peak shift is interpreted to mean the formation of solid solution of TiC and TiN. TiC and TiN both have the same NaCl type lattice and are mutually soluble. The peak shift is taken to be indicative of the formation of compounds of the type Ti(CN). The Titanium peak at a 2θ of 38.38° is due to the preliminary deposition of Ti on the substrate prior to the deposition of the TiN compound with reactive sputtering. The observation of the Ti peak suggests that the initial layer deposited has not been fully transformed to the more stable compound. A peak shift has not been observed for the principal peak of TiN 200. The data suggests that the Ti(CN) formation is not unambiguous.

Machining Tests

All the machining tests were carried out such that for each cutting condition there was one uncoated carbide tested for comparison. As seen from Figure 13 as the surface speed decreased so did the depth of the crater for the uncoated tools. All of the sputter coated tools performed well and had very small crater wear even when the test was run almost three times longer (see Table 7). Figure 14 shows the crater wear of an uncoated carbide machined for 4 min, 13 sec at a surface speed of 106.7 meters per minute. Figure 15 shows a coated carbide with almost no crater wear

Table 7. Crater Wear Results of the Machining Tests with the Coated and Uncoated Tungsten Carbide Tools. Depth of cut was 1.5 mm, feed was 0.135 mm/rev and the surface length (SL) machined was 460 meters except when noted otherwise.

Surface Speed, meters/minute	Tool	Crater Depth, microns
	Uncoated Carbide	36.8
86.4	S2	8.4
	S3	5.7
	Uncoated Carbide	41.4
89.1	S7	19.1
	S8	16.0
	Uncoated Carbide	45.0
91.8	S4	2.5
	S6	18.3
92.7[1]	S4	0.0
	Uncoated Carbide	52.1
94.5	S2	5.7
	S3	10.9
100.0	Uncoated Carbide	49.5
	S8	15.9
102.4	Uncoated Carbide	54.0
103.3[2]	Uncoated Carbide	61.6
103.3	S7	18.3
	Uncoated Carbide	57.4
106.7	S4	0.0
	S6	17.8
150.9[3]	S4	20.3

[1] SL = 1150 meters

[2] SL = 500 meters

[3] SL = 1110 meters

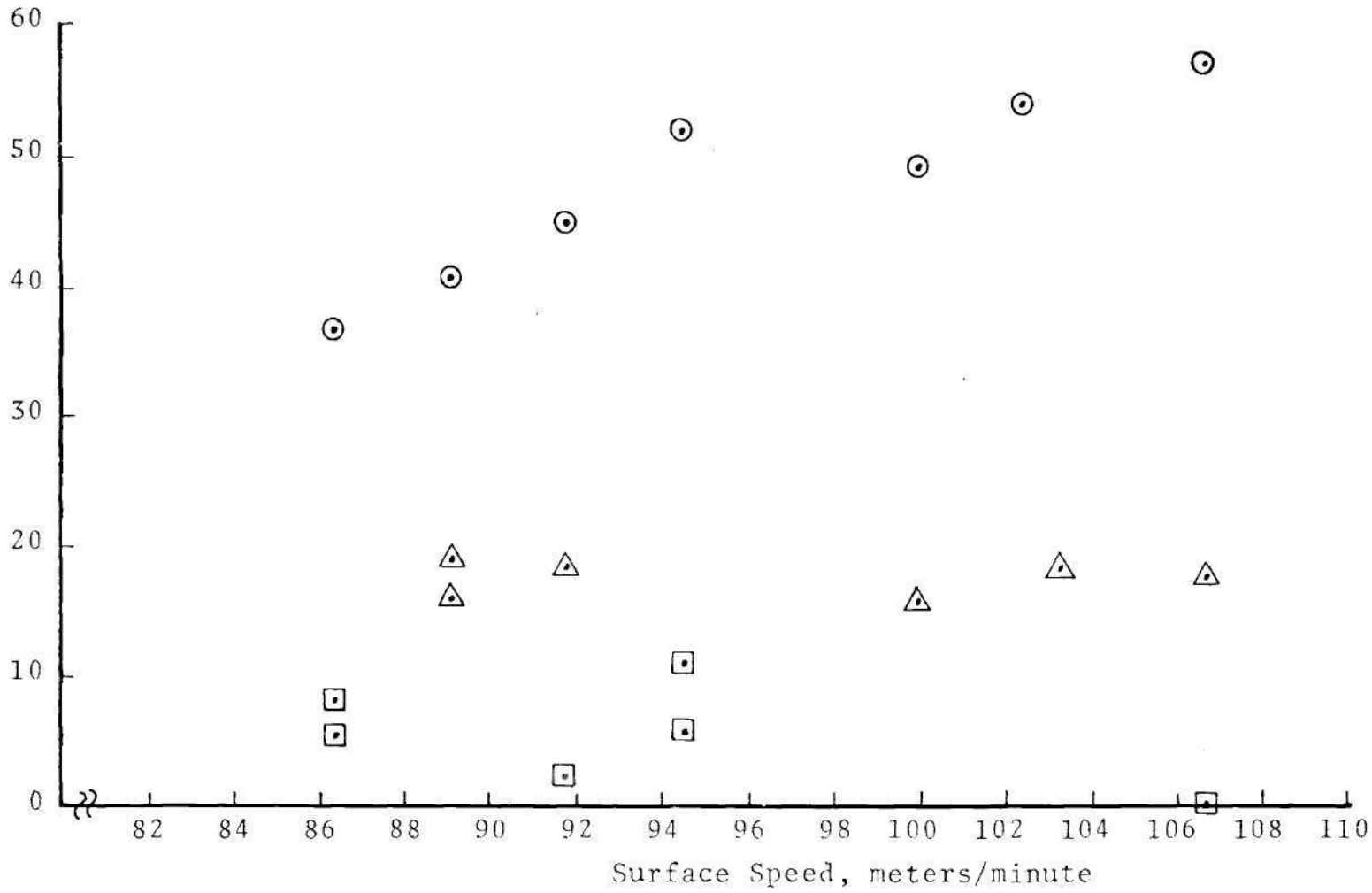

Figure 13. Crater Wear as A Function of Machining Surface Speed.

⊙ Uncoated Tungsten Carbide Tool; ⊡ Coated Tungsten Carbide Tool, Deposition Run 1; △ Coated Tungsten Carbide Tool, Deposition Run 2.

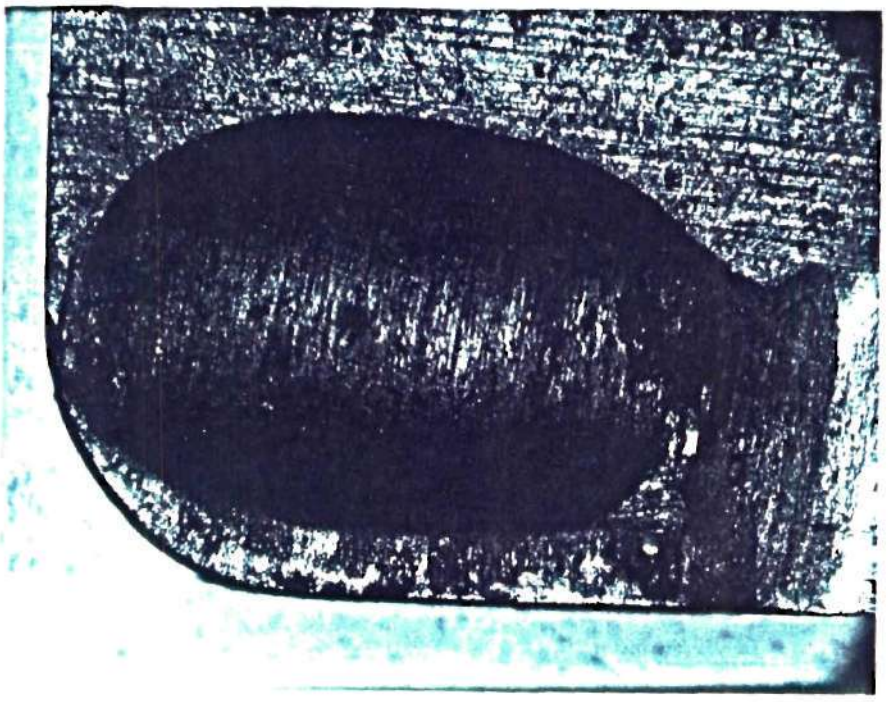

Figure 14. Crater Wear of an Uncoated Tungsten Carbide Tool Machined for 4 Minutes, 13 Seconds at a Surface Speed of 106.7 Meters per Minute

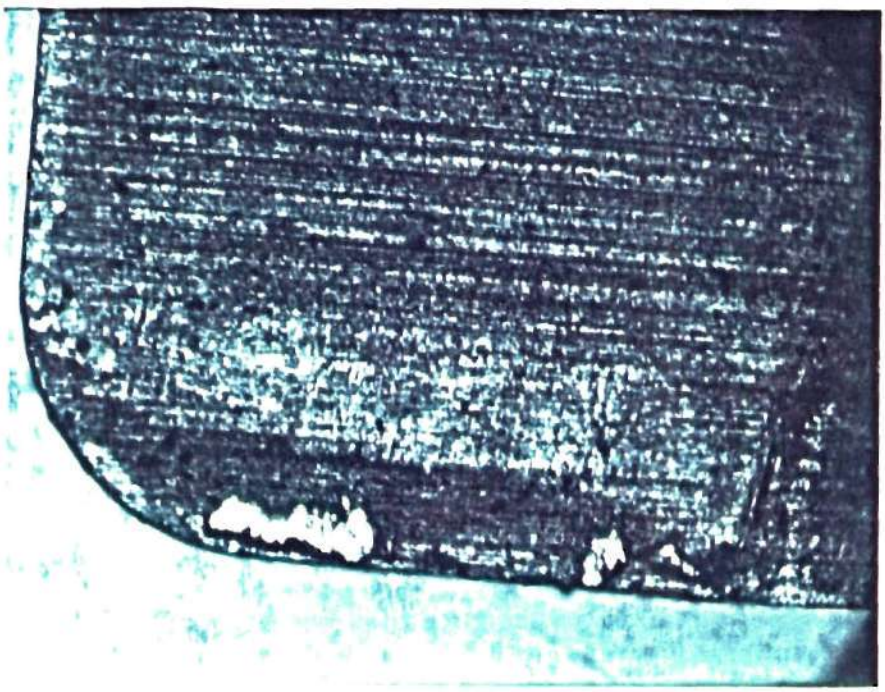

Figure 15. Coated Tungsten Carbide Tool, S4, Machined for 4 Minutes, 13 Seconds at a Surface Speed of 106.7 Meters per Minute

machined under approximately the same conditions. Figure 16 shows a coated carbide without any crater wear machined under approximately the same cutting speeds but for machining time of 12 minutes, 24 seconds. Figure 17 shows a coated carbide which was machined at a surface speed of 150.9 meters per minute for 7 min, 21 sec. This indicates that not only is the coating a hard wear resistant material, but also that it has excellent adhesion.

During the machining with the uncoated carbide tools the chips were dark blue and sparking was observed. When machining with the coated carbide tools the chips were brown and no sparks formed. This might indicate that the heat generated due to friction between the tool and work piece is less for the coated carbide which would indicate a lower friction coefficient for the coated carbide. This observation agrees with earlier findings about TiN coatings having lower friction coefficients then carbide tools.

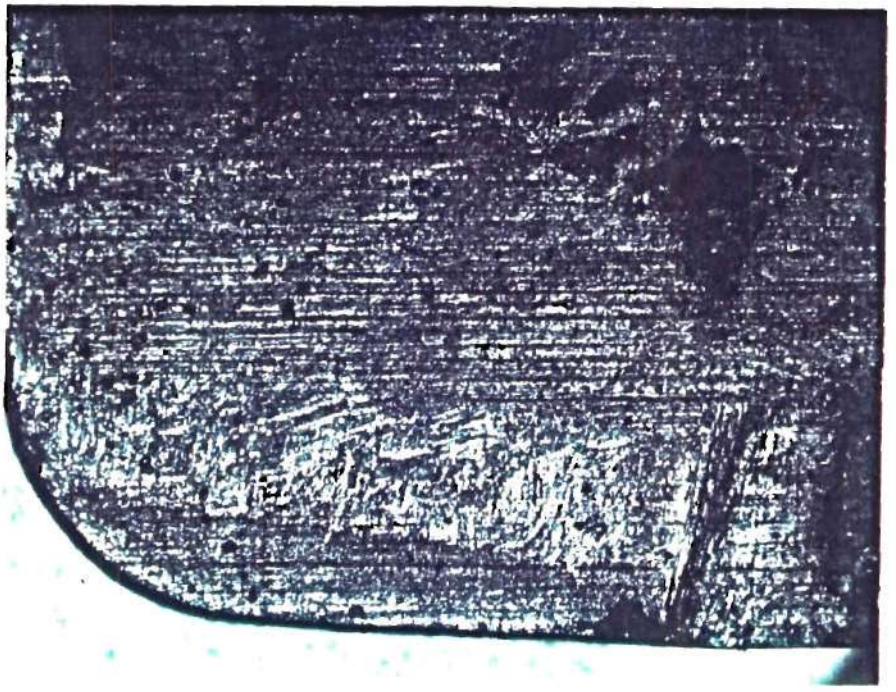

Figure 16. Coated Tungsten Carbide Tool, S4, Machined for 12 Minutes, 24 Seconds at a Surface Speed of 92.7 Meters per Minute

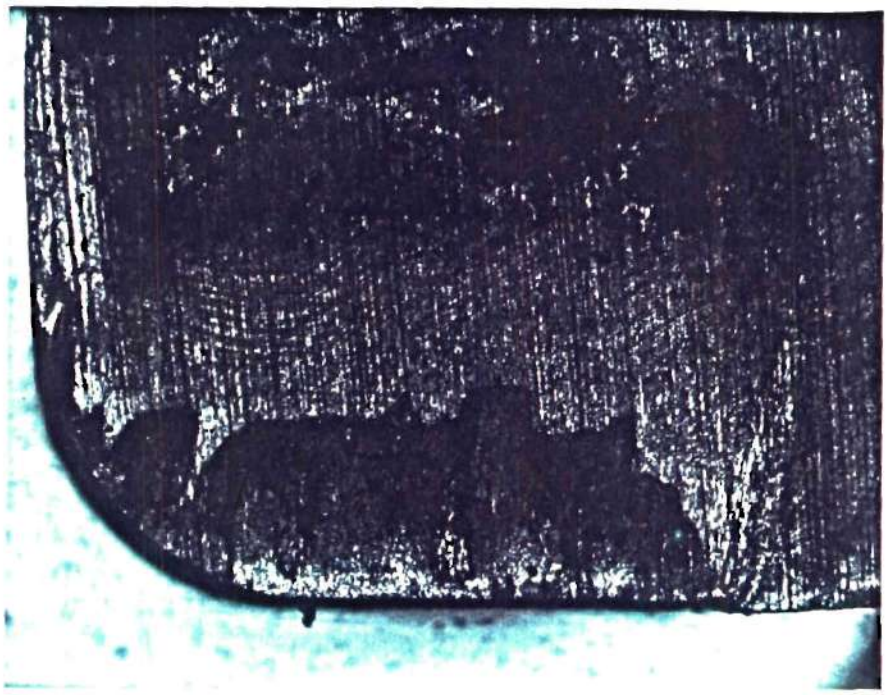

Figure 17. Wear of a Coated Tungsten Carbide Tool, S4, Machined for 7 Minutes, 21 Seconds at a Surface Speed of 150.9 Meters per Minute

CHAPTER V

CONCLUSIONS

The conclusions which can be drawn from this study are summarized as follows:

1. The planar magnetron system can be used to obtain high rate sputtering of titanium. The deposition rates and uniformity are very dependent on the target geometry and dimension.

2. The planar magnetron system can be used effectively for the formation of TiN by reactive sputtering without any additional heat treatment.

3. The reduced field is an important parameter in the formation of TiN by magnetron reactive sputtering. The reduced field can be used to predict the proper sputtering conditions and substrate location for the formation of TiN.

4. High deposition rates of TiN are conceivable with the magnetron system, but at a lower rate than sputtering titanium in an argon environment. The higher deposition rates of TiN are believed to correspond to the lower percentage of nitrogen.

5. Tool life in cutting can be increased when the tool is coated with TiN by magnetron reactive sputtering.

The substrate material is not limited to tungsten carbide.

6. The adhesion of the coatings obtained by magnetron reactive sputtering system is high enough to allow the machining of metals without decohesion of the deposited films.

Practical Application

The application of the magnetron sputtering system is not limited by substrate material, target metal, or reactive gas type. The technique can be used for coating cutting tools, ball bearings, turbine blades, or for the deposition of films used for electronic circuitry. The system can easily be arranged to fit a continuous in-line production system or a high quantity batch system. By using relative motion between the substrate and cathode, substrates of complex geometry such as drill bits, milling cutters, etc, could be coated.

Other applications which are possible include the formation of non-stoichiometric films for different film properties. The location of the substrate for the formation of the desired film could be predicted from the reduced field.

The films that are deposited need no additional finishing. They do not require any heat treatment and the surface roughness of the material after deposition is approximately the same as the material before deposition.

Suggestions for Continued Research

The efficient application of titanium nitride coatings by magnetron reactive sputtering requires that a more complete parametric study of the sputtering system be performed. One study should include the deposition rate of TiN as a function of percent nitrogen in the sputtering environment. Also, film thickness distribution should be improved and studied for the effect the system design change has on the formation of TiN. In addition to machining tests, friction and adhesion studies should be done on the TiN coatings obtained by magnetron reactive sputtering.

APPENDICES

APPENDIX A

Material Machined:

U.S. Steel, Heat No. B97710.

Grade AISI 1045, fine grained.

Chemical Analysis, in percent

C	Mn	P	S	Si	Fe
0.45	0.80	0.016	0.034	0.19	98.57

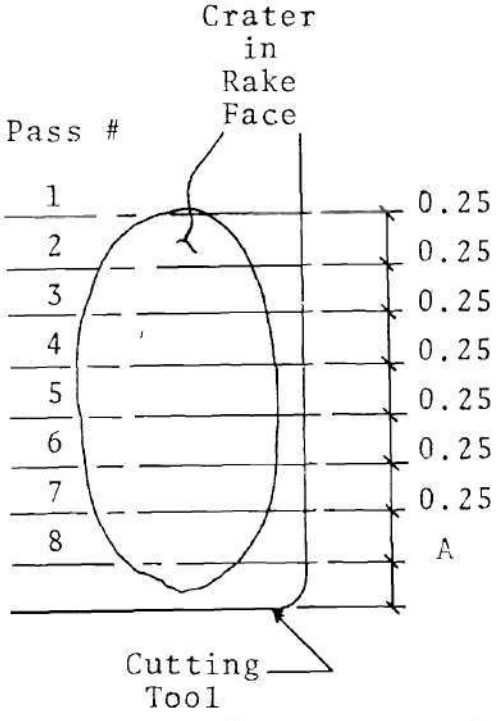

Location of Crater Depth Profiles Measured by a Profilometer on Cutting Tool. (Units in mm)

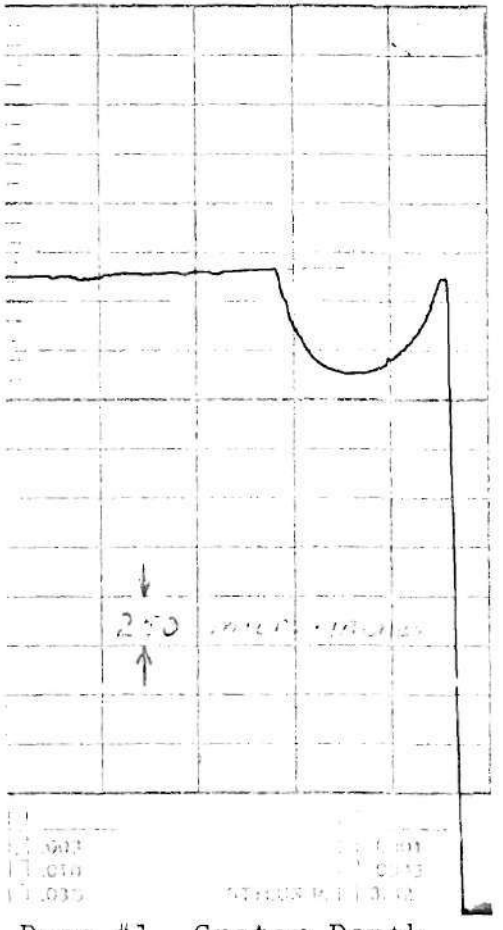

Pass #1, Crater Depth is 650 micro-inches

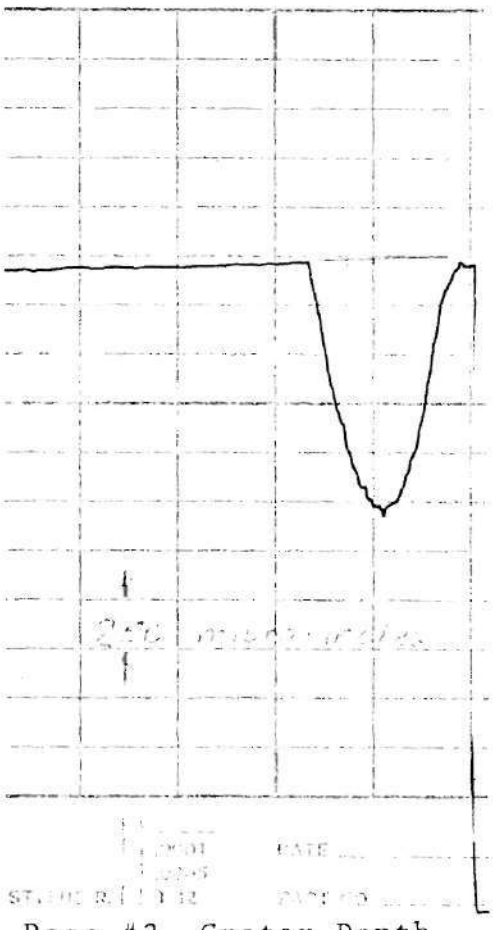

Pass #2, Crater Depth is 1300 micro-inches

Crater Depth Measurements by Profilometer of a Uncoated Tungsten Carbide Tool Machined at a Surface Speed of 106.6 meters/minute for 4 minutes, 13 seconds.

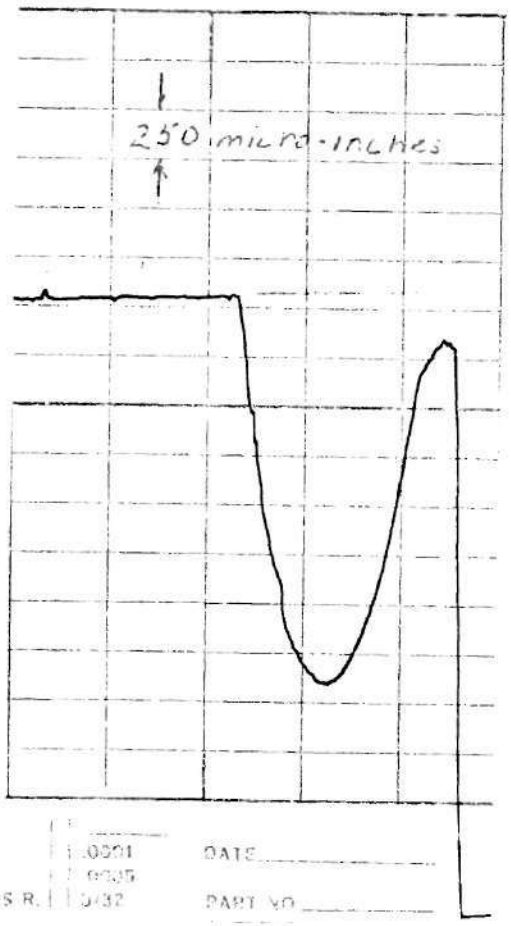

Pass # 3, Crater Depth is 2060 micro-inches.

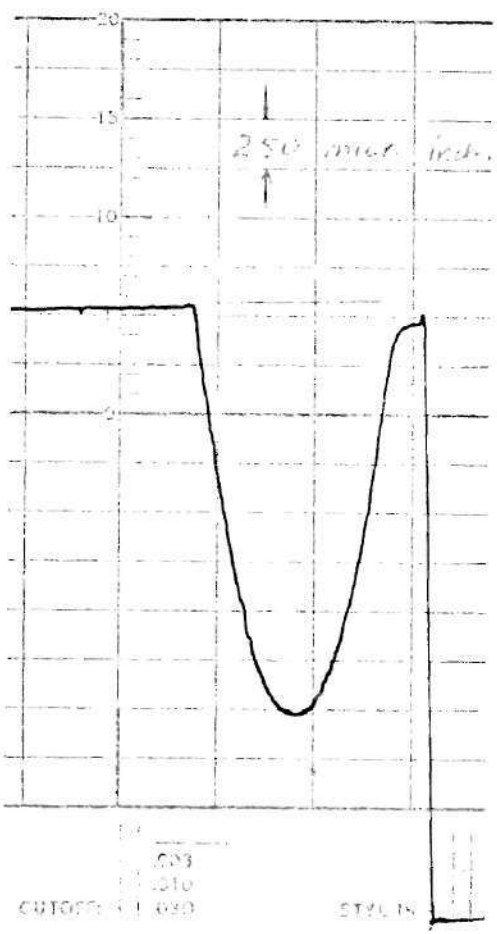

Pass #4, Crater Depth is 2100 micro-inches.

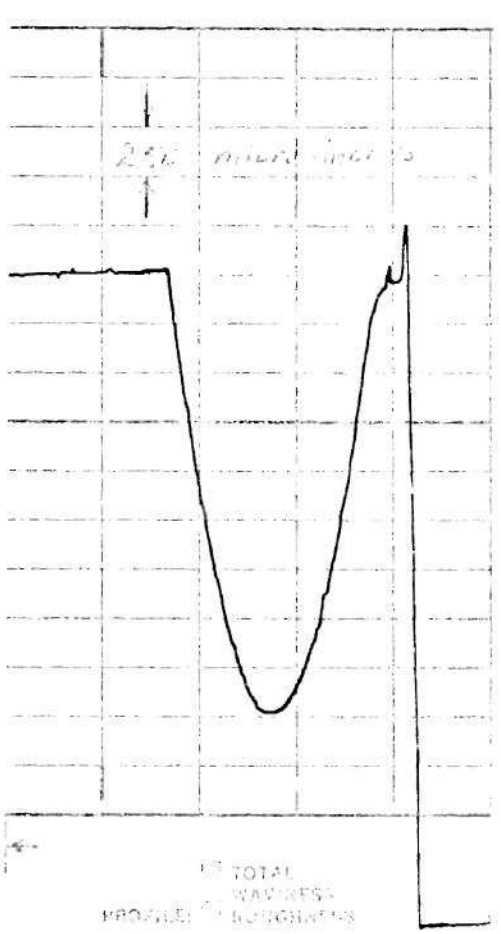

Pass #5, Crater Depth is 2260 micro-inches

Crater Depth Measurements by Profilometer of a Uncoated Tungsten Carbide Tool Machined at a surface speed of 106.6 meters/minute for 4 minutes, 13 seconds.

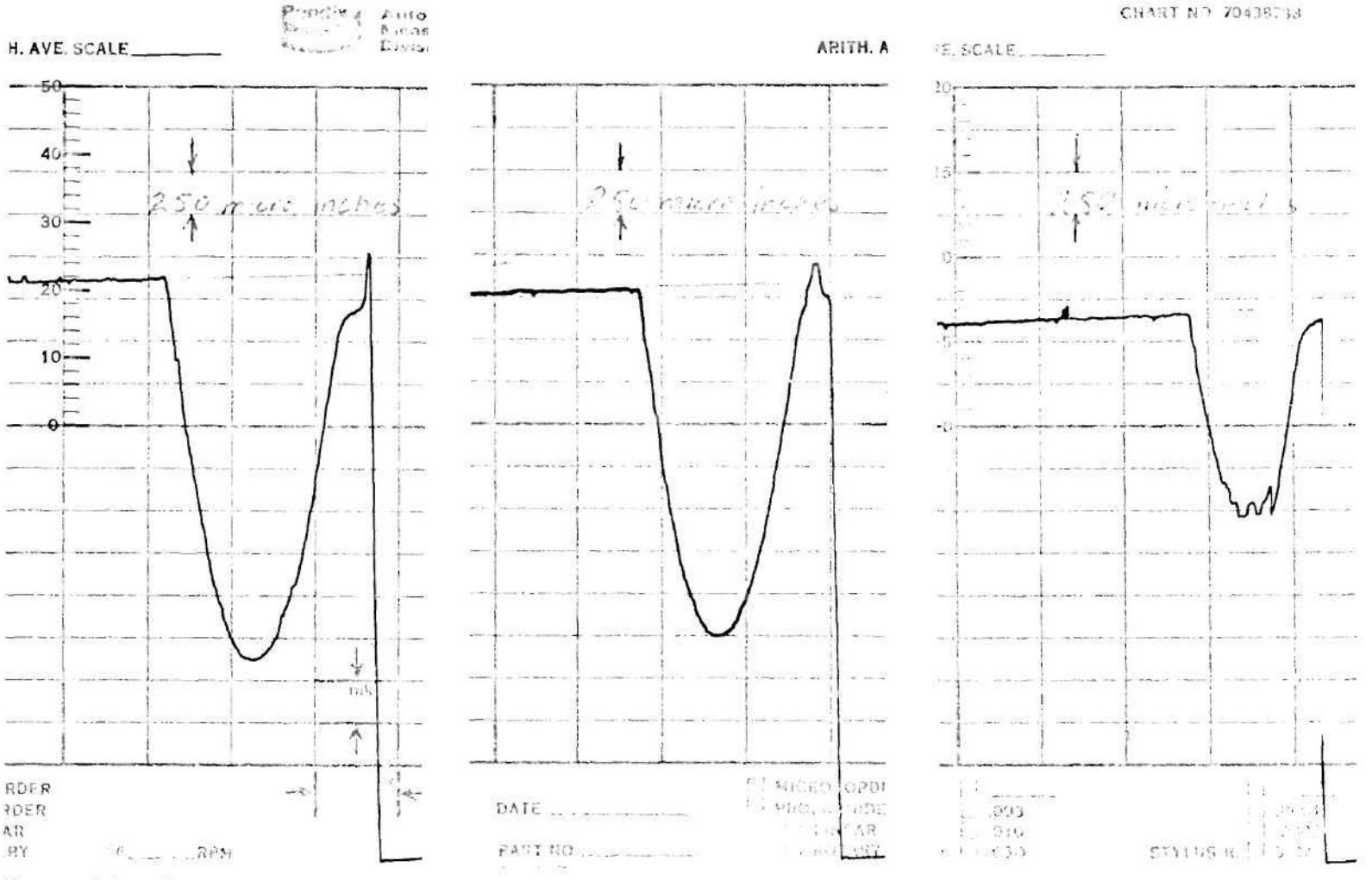

Pass #6, Crater Depth is 2260 micro-inches

Pass #7, Crater Depth is 2060 micro-inches

Pass #8, Crater Depth is 1175 micro-inches. A=0.27mm.

Crater Depth Measurements by a Profilometer of a Uncoated Tungsten Carbide Tool Machined at a surface speed of 106.6 meters/minute for 4 minutes, 13 seconds.

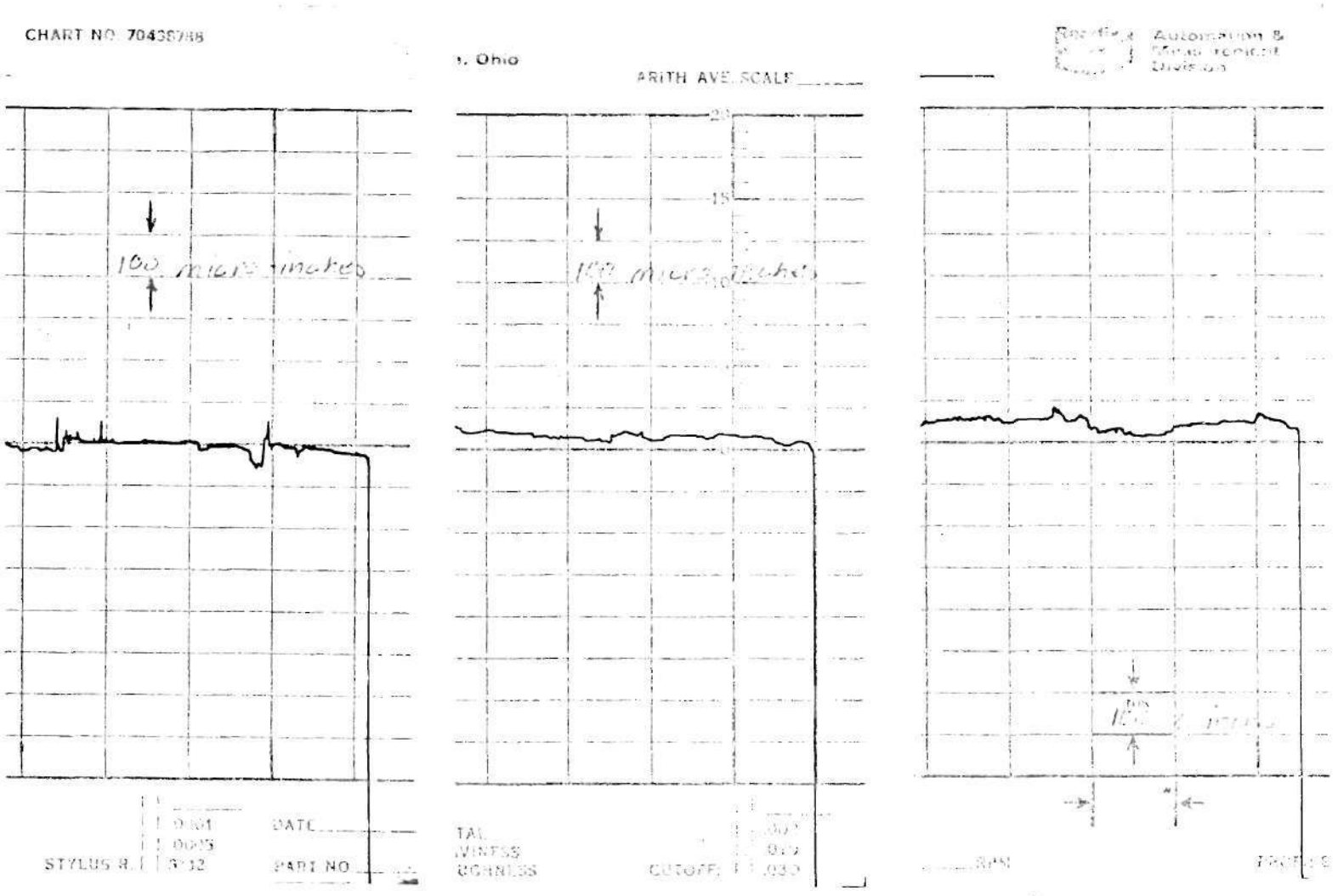

Pass #1, No Crater Pass #2, No Crater Pass #3, No Crater

Crater Depth Measurements by Profilometer of Coated Tungsten Carbide Tool, S4, machined at a surface speed of 106.6 meters/minute for 4 minutes, 13 seconds.

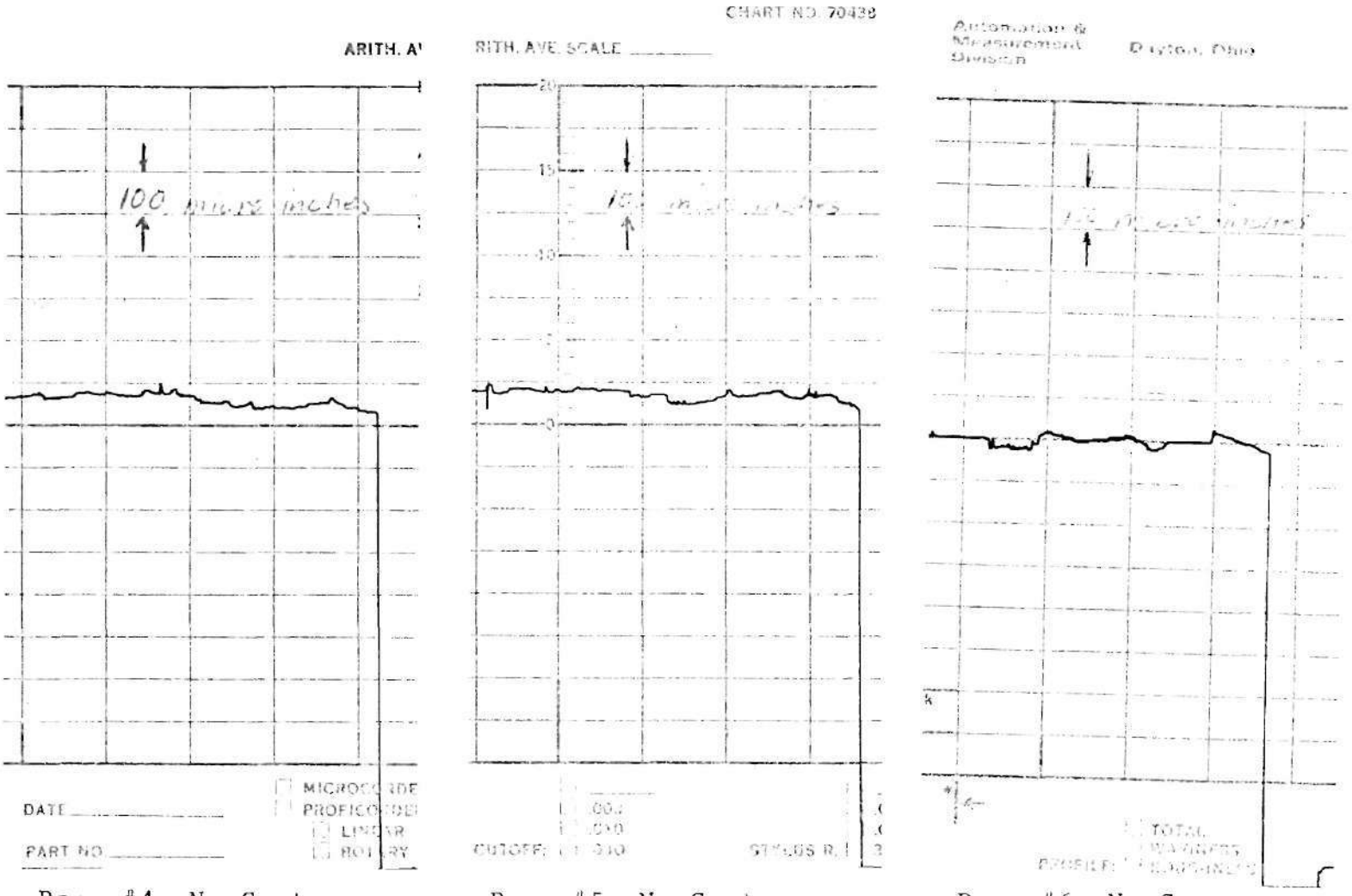

Pass #4, No Crater Pass #5, No Crater Pass #6, No Crater

Crater Depth Measurements by Profilometer of Coated Tungsten Carbide Took, S4, machined at a surface speed of 106.6 meters/minute for 4 minutes, 13 seconds.

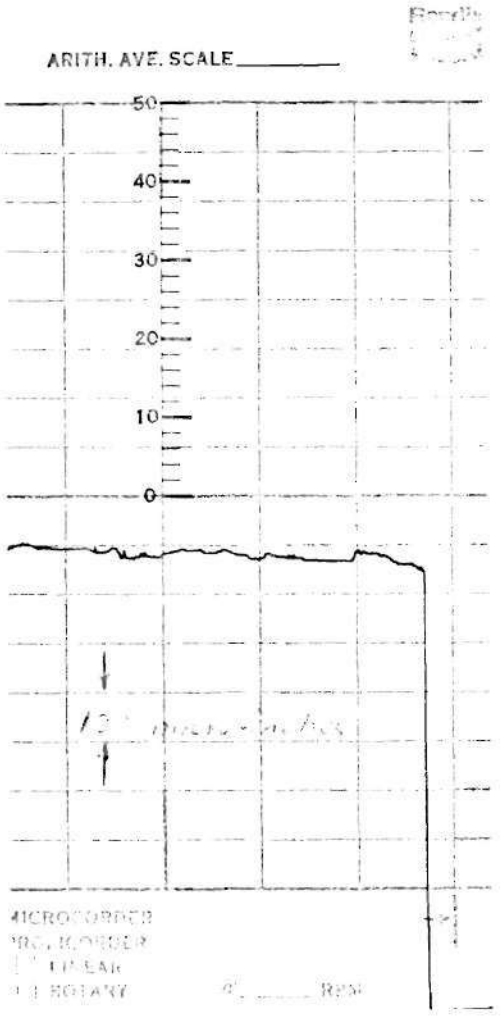

Pass #7, No Crater

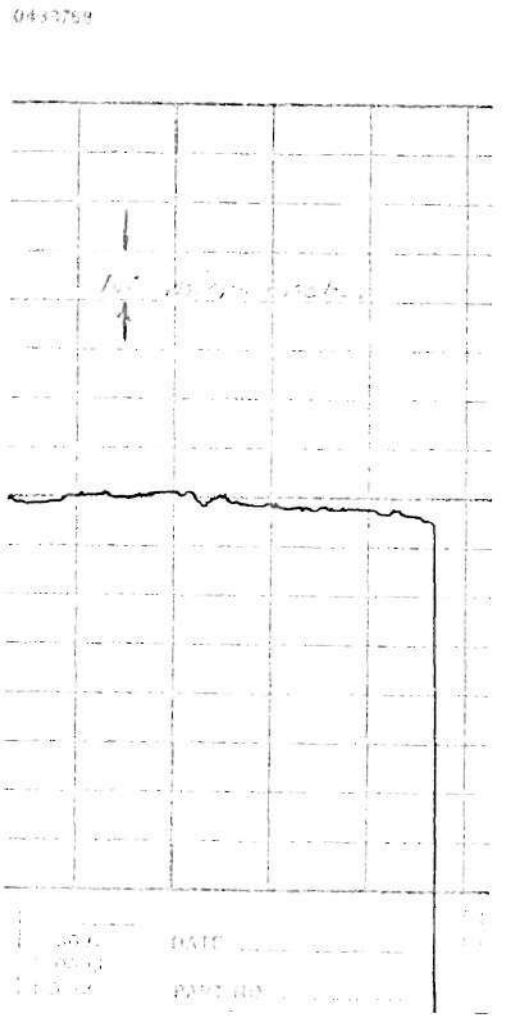

Pass #8, No Crater, A=0.1mm.

Crater Depth Measurements by Profilometer of Coated Tungsten Carbide Tool, S4, machined at a surface speed of 106.6 meters/minute for 4 minutes, 13 seconds.

BIBLIOGRAPHY

1. Mukherjee, J. L., Wu, L. C., Greene, J. E., and Cook, H. E., Journal of Vacuum Science Technology, 12, p. 850, 1975.

2. Metals and Materials, p. 38, Oct. 1976.

3. Yee, K. K., International Metal Reviews, 1, p. 19, 1978.

4. Stjernberg, K. G., Thin Solid Films, 40, p. 81, 1977.

5. Kieffer, R., Fister, D., Schoof, H., and Mauer, K., Powder Metallurgy International, 5, p. 188, 1973.

6. Itoh, A., Proceedings of the Fourth International Vacuum Congress, Part II, p. 536, 1968.

7. Bunshah, R. F. and Ragharam, A. C., Journal of Vacuum Science Technology, 9, p. 1385, 1972.

8. Nakamura, K., Inagawa, K., Tsuruoka, K., and Komiya, S., Thin Solid Films, 40, p. 155, 1977.

9. Bunshah, R. F., Shabaik, A. H., Nimmagadda, R., and Covy, J., Thin Solid Films, 45, p. 453, 1977.

10. Clarke, P. J., Journal of Vacuum Science Technology, 14, p. 141, 1977.

11. Murayama, Y., Journal of Vacuum Science Technology, 12, p. 818, 1975.

12. Mah, G., Nordin, C. W. and Fuller, J. F., Journal of Vacuum Science Technology, 11, p. 371, 1974.

13. Cook, N. A. and Su, K. Y., Proceedings of the Fifth North American Metalworking Research Conference, p. 297, 1977.

14. Greene, J. E. and Pests, M., Thin Solid Films, 37, p. 375, 1976.

15. Wu, L. C., Zillco, J. L., Mukherjee, J. L., Greene, J. E., and Cook, H. E., The International Conference of Wear of Materials, p. 364, 1977.

16. Carson, W. W., Journal of Vacuum Science Technology, 12, p. 845, 1975.

17. Thorton, J. A., Journal of Vacuum Science Technology, 15, p. 171, 1978.

18. Schiller, S., Heisig, U., and Goedicke, K., Journal of Vacuum Science Technology, 14, p. 815, 1977.

19. Aronson, A. and Weinig, S., Vacuum, 27, p. 157, 1977.

20. Grove, W. R., Transaction Royal Society (London), 42, p. 87, 1852.

21. Berry, R. W., Hall, P. M., and Harris, M. T., Thin Film Technology, D. Van Nostrand Company, Inc., p. 201, 1968.

22. Maissel, L. I. and Clang, R., Handbook of Thin Film Technology, McGraw-Hill, 1970.

23. Seeliger, R. and Sommermeyer, K., Zeits. f. Physik, 93, p. 692, 1935.

24. Fetz, H., Zeits, f. Physik, 119, p. 590, 1942.

25. Wehner, G. K., Journal of Applied Physics, 25, p. 270, 1954.

26. Wehner, G. K., Physical Review, 102, p. 690, 1956.

27. Wehner, G. K., Journal of Applied Physics, 30, p. 1762, 1959.

28. Bradley, R. C., Physical Review, 93, p. 719, 1954.

29. Thompson, U. W., Philosophy Magazine, 4, p. 139, 1959.

30. Anderson, G. S. and Wehner, G. K., Journal of Applied Physics, 31, p. 2305, 1960.

31. Laegried, N. and Wehner, G. K., Journal of Applied Physics, 32, p. 365, 1961.

32. Rosenberg, D. and Wehner, G. K., Journal of Applied Physics, 32, p. 887, 1961.

33. Almen, O. and Bruce, G., Nuclear Instrumentation and Methods, 11, p. 279, 1961.

34. Wehner, G. K., Advances in Electronics and Electron Physics, Vol. VII, p. 292, 1955.

34. Wehner, G. K., Advances in Electronics and Electron Physics, Vol. VII, p. 292, 1955.

35. Kaminsky, M., Atomic and Ionic Impact Phenomena on Metal Surfaces, Academic Press, Inc., 1965.

36. Carter, G. and Colligon, J. S., Ion Bombardment of Solids, Amer. Elsevier Publishing, Inc., 1968.

37. Schwartz, N., Amer. Vac. Soc., Transactions on the Tenth National Vacuum Symposium, p. 325, 1963.

38. Abe, T. and Yamashina, T., Thin Solid Films, 30, p. 19, 1975.

39. Itoh, A. and Shinoki, F., Journal of Applied Physics, 46, p. 3381, 1975.

40. Campbell, D. S. and Hollands, E., Journal of Material Science, 3, p. 544, 1968.

41. Hobson, J. P. and Redhed, P. A., Proceedings of the Fourth International Vacuum Congress, p. 3, 1968.

42. Penny, G. and Martin, B. L. S., Proceedings International Symposium, Clausthal, 1965, Vandenhoeck and Ruprecht, Goettingen, 1966.

43. Perny, G., Martin, B. L. S., and Samirant, M., Compt. Rend., 263, p. 265, 1966.

44. Perny, G., Vide, p. 106, Oct. 1966.

45. Penning, S. M. and Moubis, J. H. A., Proc. Koninkl. Ned. Akad. Wefenschap., 43, p. 41, 1940.

46. Chapin, J. S., Research/Development, 37, 1975.

47. Kirov, K. I., Georgiev, S. S., Ivanoy, and Minchev, G. M., Vacuum, 28, p. 183, 1978.

48. Van Esdonk, J. and Janssen, J. F. M., Research/ Development, p. 41, Jan. 1975.

49. Schiller, S., Heisig, U., and Goedicke, K., Thin Solid Films, 40, p. 327, 1977.

50. Ball, D. J., Journal of Applied Physics, 43, p. 3047, 1972.

51. Waits, R. K., Journal of Vacuum Science Technology, 15, p. 178, 1978.

52. Ramalingam, S. and Faulring, G., Proceedings of the Sixth North American Metalworking Research Conference, p. 290, 1978.

53. Byrd, J. D. and Ferguson, B. L., Proceedings of the Sixth North American Metalworking Research Conference, p. 310, 1978.

54. Williams, W., Proc. of V NSF Hard Materials Workshop, Providence, R.I., 1977.

55. Trent, E. M., Metal Cutting, Butterworths, 1977.

56. Cook, N. H. and Nayak, P. N., Journal of Engineering for Industry, p. 93, Feb. 1966.

57. Cook, N. H., Journal of Engineering for Industry, p. 931, Nov. 1973.

58. Schwarzkopf, P. and Kieffer, R., Refractory Hard Metals, The MacMillan Co., p. 233, 1953.

59. Mittal, K. L., Electrocomponent Science and Technology, 3, p. 21, 1976.

60. Moeller, T., Inorganic Chemistry, John Wiley & Sons, Inc., New York, 1952.